BELT OROGENESIS ALONG THE NORTHERN MARGIN OF THE IDAHO BATHOLITH

Charles S. Hutchison

Idaho Bureau of Mines and Geology
Department of Lands
Moscow, Idaho 83843

IBMG Open-File Report 81-2
This report is preliminary
and may be modified later.
April 1981

TABLE OF CONTENTS

LIST OF TABLES

LIST OF FIGURES

BELT OROGENESIS ALONG THE NORTHERN MARGIN OF THE IDAHO BATHOLITH

by

Charles S. Hutchison[1]

ABSTRACT

The Belt succession of the Clearwater National Forest along the northern margin of the Idaho batholith extends upward from massive white metaquartzite of the Burke and Revett Formations to quartz-oligoclase gneisses and garnet-quartz-mica schists of the St. Regis Formation and then to the thinly interbedded white saccharoidal metaquartzite, green diopside-calcite-oligoclase gneiss, and brown phlogopite-oligoclase gneiss of the Wallace Formation, which also contains a prominent thick garnet-quartz-mica schist unit.

Beltian sedimentation began about 1,500 m.y. ago in an aulacogen on the edge of the North American craton. Basic sills, emplaced during the extensional development of the aulocogen, were later isoclinally folded together with the Belt sediments and metamorphosed to amphibolite. F_1 deformation and metamorphism of the sediments is dated at 1,200 m.y., but the grade attained cannot be ascertained because of preponderant Mesozoic and Cenozoic plutonism and metamorphic recrystallization.

Idaho batholith granitoid emplacement culminated at 70 to 80 m.y. and was related to subduction of the Pacific plate beneath the craton.

[1]Department of Geology, University of Malaya, Kuala Lumpur 22-11, Malaysia.

Diabase and rhyodacite sills of Eocene age widely intruded the metasediments, and granitoids were extensively emplaced in the batholiths, causing a resetting of most of the older isotope dates to 50 m.y. or younger. Extensive pegmatite subcordant intrusions into the metasediments are considered synchronous with the batholith.

The sillimanite grade of the Belt metasediments appears to have crystallized during the Mesozoic-Cenozoic orogeny, and earlier metamorphic events have been overprinted. The folding complexity indicates three deformations. The F_1 isoclinal folds were dispersed during an F_2 folding event, for which details cannot be uniquely deduced. The late-stage F_3 folding gave a large northeast-plunging syncline which dominates the outcrop pattern.

INTRODUCTION

Precambrian supracrustal rocks, deposited between 1,700 and 850 m.y., form scattered fault-bounded troughs dispersed on the North American craton. The largest of these troughs, which are inferred to have been fault-bounded at least on one side, are the Belt-Percell and Keweenawan that contain sedimentary and volcanic piles more than 15,000 meters thick (Stewart, 1976). The strata are associated with mafic intrusive and extrusive igneous rocks that suggest widespread extension. The troughs are not confined to the cratonic margins, whereas miogeosynclinal strata were deposited peripherally around the craton from 850 to 540 m.y. (Stewart, 1976).

The Belt basin represents a slowly subsiding re-entrant on the western edge of the craton, beginning about 1,500 m.y. and persisting until about 900 m.y. The basin was not strictly graben shaped and at times in its development had a triangular outline (Figure 1). Harrison and others (1974) drew attention to its resemblance to an aulacogen. Sears and Price (1978) accepted the hypothesis and matched the Belt basin with a counterpart on the edge of the Siberian craton. These aulacogens formed as the Archean craton split up about 1,500 m.y. into the North American craton and the Siberian platform, and the aulacogens so formed were filled with supracrustal rocks as the sectors progressively separated.

The western limit of the North American craton can be taken as the limit of Precambrian outcrops (Armstrong, 1975; Harrison and others, 1974). It may also be more precisely defined as the line of 0.704 initial $^{87}Sr/^{86}Sr$ isotope ratios for Cordilleran plutonic igneous rocks of Mesozoic and Cenozoic age (Armstrong and others, 1977). Isotope ratios west of this line grade downwards to 0.702, indicating the absence of continental basement (Figure 1). East of the line the ratios increase to 0.707, and the major Mesozoic batholiths, including the Idaho batholith, lie just east of the 0.704 line (Figure 1). This line undoubtedly represents the Mesozoic plate margin, as required by the distribution of the Cordilleran mineral deposits (Guild, 1978).

The deformation and metamorphic history of the Belt rocks is far from resolved. Metamorphic grade increases with stratigraphic depth. The increase in burial depth from Montana westward toward Idaho has caused a transformation in the 1Md to the 2M illite polymorph. This transformation is completed at the biotite isograd (Maxwell and Hower, 1967).

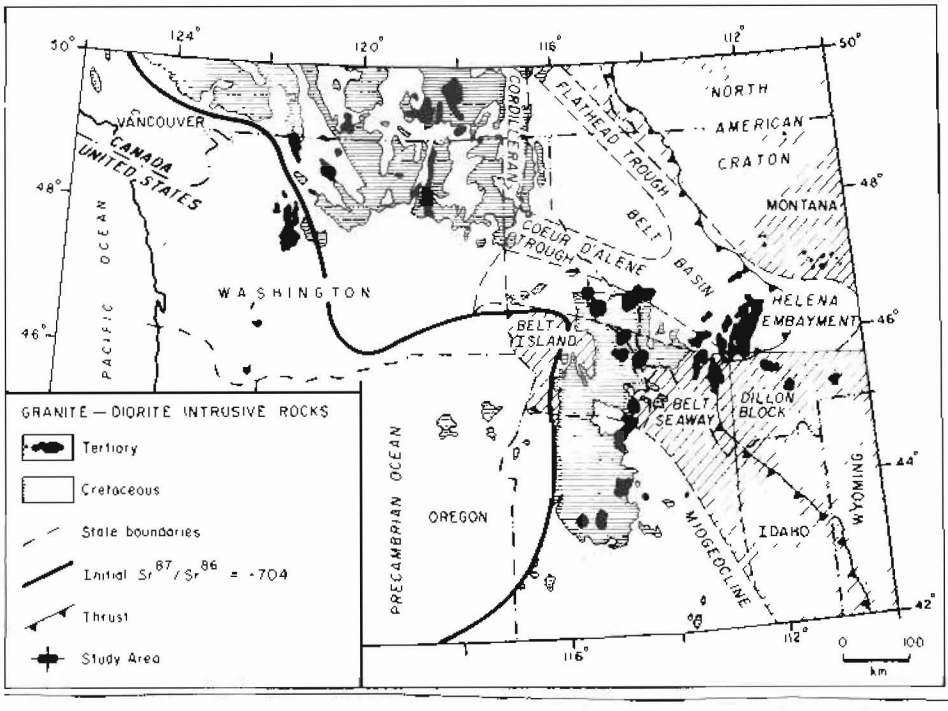

Figure 1. Principal tectonic elements of the Belt aulacogen (after Harrison and others, 1974), showing also the $^{87}Sr/^{86}Sr$ isotope ratio line of 0.704 (after Armstrong and others, 1977) for Mesozoic-Cenozoic igneous rocks that define the western margin of the North American craton.

There is also a much more spectacular increase of metamorphic grade toward the Idaho batholith (Hietanen, 1967). The line of the Mesozoic batholiths coincides with the zone of greatest thickness of the Belt Series; and since the highest grades coincide with the lower stratigraphic units, it becomes necessary to use a model of increasing grade with depth of burial in the Precambrian. This metamorphism was overprinted by higher geothermal gradients and deformation toward the line of the batholith during the Mesozoic-Cenozoic Era (Figure 2). Radiometric dating revealed that the metamorphic paragenesis of sillimanite, kyanite, and staurolite recrystallized in the period 40 to 64 m.y., but the ages increase abruptly to 200 m.y. in the garnet and to 430 m.y. in the biotite zone (Hofmann, 1972).

The Idaho batholith was emplaced within the period 70 to 84 m.y.; however, minor igneous activity extends back from the Cretaceous to the Paleozoic (Armstrong and others, 1977). A series of large Tertiary plutons (Figure 1) and associated dike swarms, intruded approximately 45 m.y., has probably reset many older batholith ages.

This paper presents the geologic study of an area of sillimanite grade Belt rocks immediately adjacent to the northern margin of the Bitterroot lobe of the Idaho batholith. The area lies 10 kilometers east of the Canyon ranger station and 15 kilometers north of the Bungalow ranger station in the Clearwater National Forest of northern Idaho, bounded by longitudes $115^{\circ}21'$ and $115^{\circ}30'$ west and latitudes $46^{\circ}45'$ and $46^{\circ}52'$ north. No detailed geologic study has been previously made, but the area is included in several reconnaissance and regional syntheses (Hietanen, 1963, 1967, 1968). A description of the areal geology is followed by a discussion of the tectonism, metamorphism, and igneous activity.

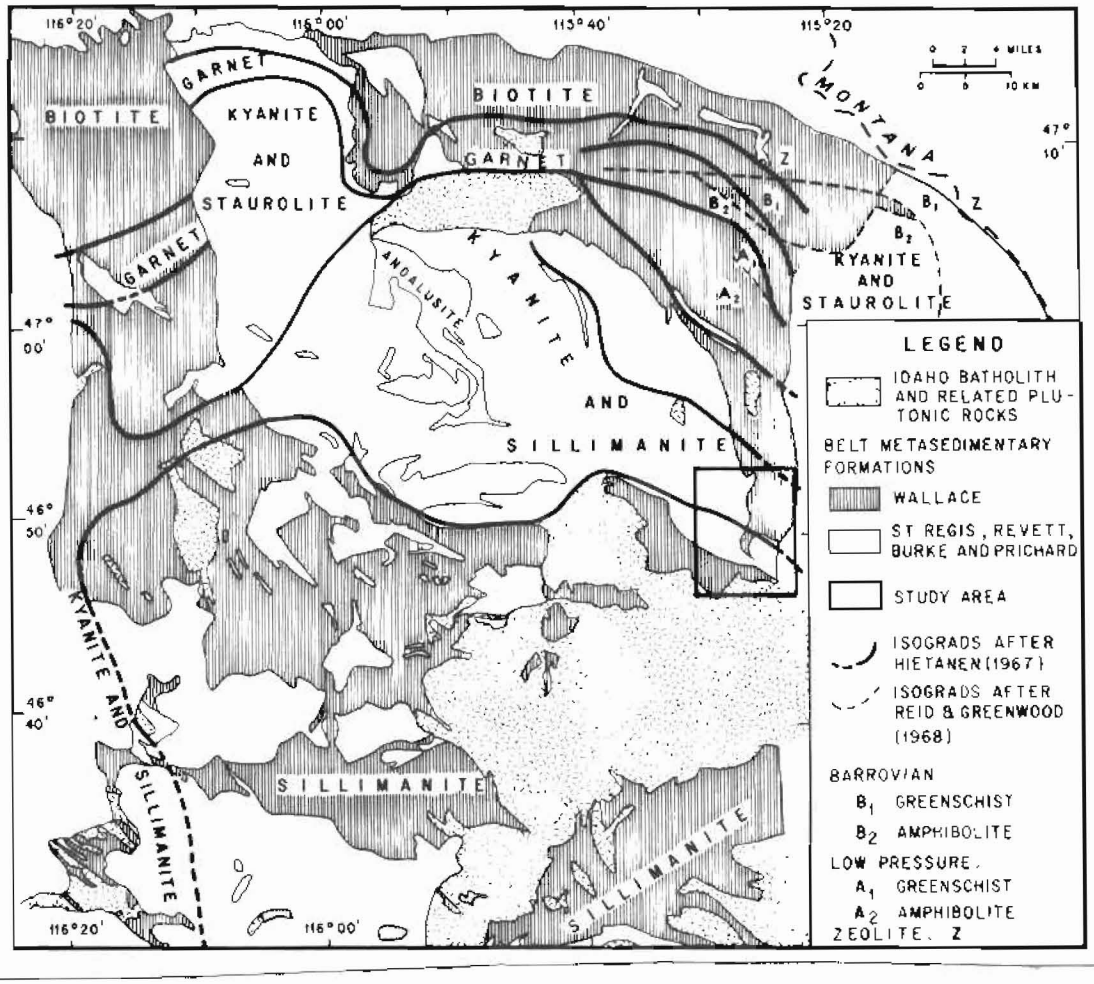

Figure 2. Simplified geological map showing the distribution of Beltian metamorphic grades in relation to the Idaho batholith (after Hietanen, 1967; Reid and Greenwood, 1968).

METASEDIMENTARY FORMATIONS

The Wallace Formation has been mapped with certainty because of its distinctive lithology (Figure 3). The underlying garnet-mica-quartz schists, the psammitic gneisses, and the metaquartzites can only be tentatively correlated with the St. Regis, Revett, and Burke Formations, following the regional characteristics given by Hietanen (1967).

BURKE FORMATION

Hietanen (1968) subdivided the Burke Formation into two units: the lower Burke Quartzite composed of 500 meters of coarse-grained, light gray to white micaceous quartzite containing schist layers; and the upper Burke Schist composed of 180 meters of garnet-mica schist. The thicknesses of Hietanen agree closely with the total of 610 meters given by Ross (1970).

Rocks tentatively ascribed to the Burke Formation (Figure 3) bear a similarity to the descriptions of Hietanen (1963, 1967, 1968). The predominant rock is a crudely foliated or massive, cream white metaquartzite containing brown weathered spots. The grain size is not discernible in hand specimen. Under the microscope the sutured quartz grains generally range from 0.4 to 0.6 millimeter (Figure 4a). Recrystallization near the Idaho batholith may have been responsible for an increase in grain size to 3 millimeters. Cataclasis is common, and crystals between 2 and 3 millimeters in diameter occur in zones parallel to the predominant foliation (Figure 4b). Most of the metaquartzite is composed of at least 90 percent sutured quartz, rare interstitial biotite, and subsidiary An_{20} oligoclase. It is interfoliated with strongly sheared gneiss containing black mica-rich schlieren and white feldspathic layers.

Figure 3. Geologic map of the study area in the Clearwater National Forest, Idaho. Diabase and rhyodacite sills have been left off for the sake of clarity (see Figure 9). Only a selection of the structural data is given. The bold arrows indicate the direction of plunge of major folds determined from the stereograms of Figure 11. The area of detailed study shown in Figure 3 comprises the whole of the 1963, 1:24,000-scale quadrangle topographic sheet, *The Nub, Idaho, N4647-W11522.5/7.5*, and the western seventh of the sheet, *Elizabeth Lake, Idaho, N4645-W11515/7.5*. The area is covered by air photographs of the 1962 series EJO of scale 1:20,000 and the 1959 series EGW-1 of scale 1:42,857.

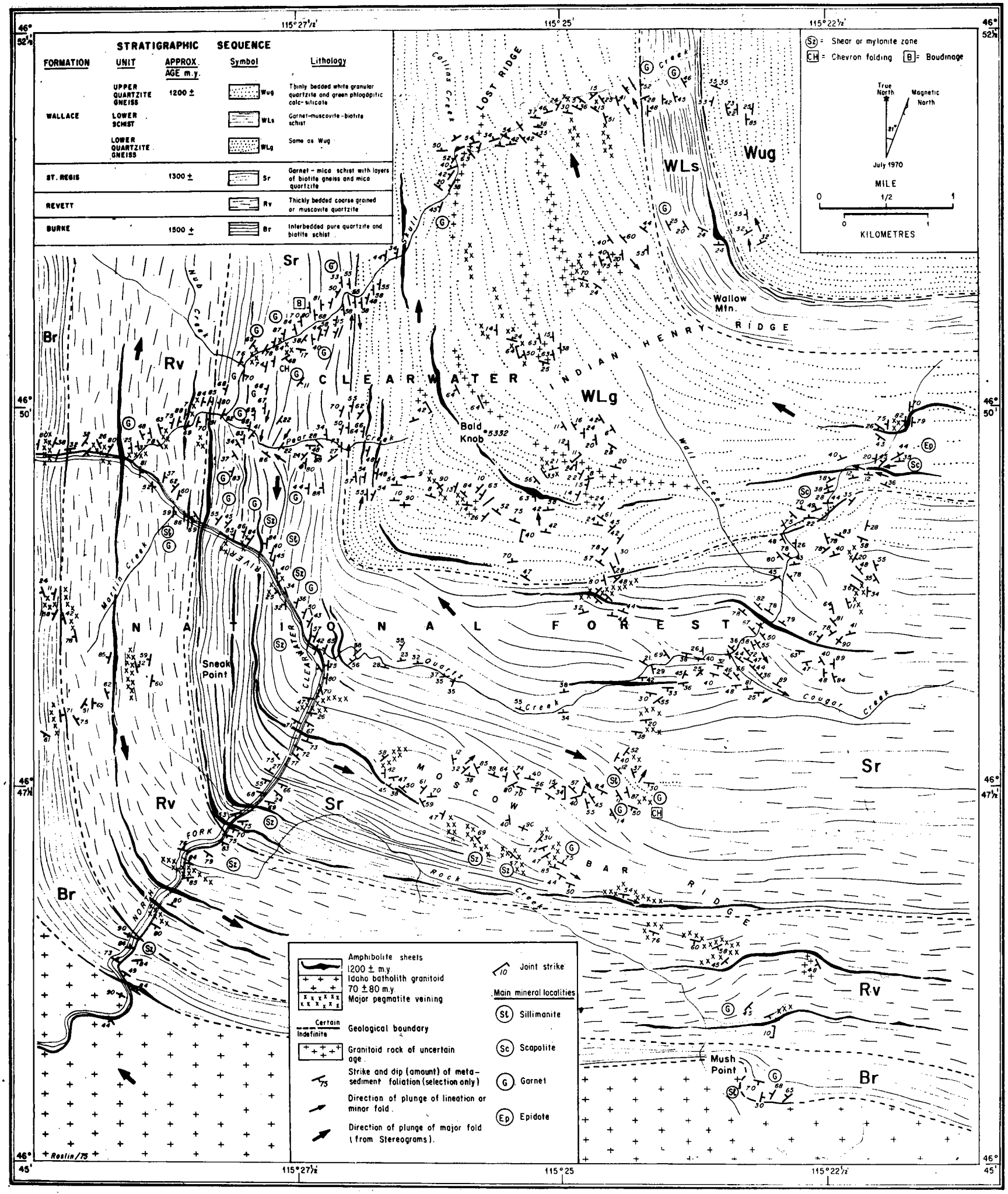
STRATIGRAPHIC SEQUENCE
FORMATION
UNIT
APPROX. AGE m.y.
Symbol
Lithology
WALLACE
UPPER QUARTZITE GNEISS
1200 ±
Wug
Thinly bedded white granular quartzite and green phlogopitic calc-silicate
LOWER SCHIST
WLs
Garnet-muscovite-biotite schist
LOWER QUARTZITE GNEISS
WLg
Same as Wug
ST. REGIS
1300 ±
Sr
Garnet – mica schist with layers of biotite gneiss and mica quartzite
REVETT
Rv
Thickly bedded coarse grained or muscovite quartzite
BURKE
1500 ±
Br
Interbedded pure quartzite and biotite schist
Sz = Shear or mylonite zone
CH = Chevron folding
B = Boudinage
True North
Magnetic North
21°
July 1970
MILE
0
1/2
1
KILOMETRES
115° 27½'
115° 25'
115° 22½'
46° 52½'
46° 50'
46° 47½'
46° 45'
LOST RIDGE
Collins Creek
Stull Creek
Wallow Mtn.
INDIAN HENRY RIDGE
CLEARWATER
Bald Knob 5332
Wall Creek
Poor Farm Creek
Martin Creek
RIVER
Sneak Point
CLEARWATER
NATIONAL FOREST
Quartz Creek
Cougar Creek
MOSCOW
Rock Creek
BAR RIDGE
NORTH FORK
Mush Point
Amphibolite sheets 1200 ± m.y.
Idaho batholith granitoid 70 ±80 m.y.
Major pegmatite veining
Certain
Indefinite
Geological boundary
Granitoid rock of uncertain age.
Strike and dip (amount) of metasediment foliation (selection only)
Direction of plunge of lineation or minor fold.
Direction of plunge of major fold (from Stereograms).
Joint strike
Main mineral localities
St Sillimanite
Sc Scapolite
G Garnet
Ep Epidote
Reslin/75

Figure 3

Figure 4. Thin-section appearance: (a) Banded metaquartzite of the Burke Formation (7639, cross-polars, from North Fork of the Clearwater River, southwest corner of map); (b) Cataclastic augen feldspathic gneiss of the Burke Formation (7642, from North Fork of the Clearwater River, southwest corner of map); (c) Biotite-feldspar-quartz gneiss of the Revett Formation (7631 from North Fork of the Clearwater River, southwest corner of map); (d) Muscovite metaquartzite of the St. Regis Formation (7597, cross-polars, from the junction of Quartz and Cougar Creeks); (e) Chevron-folded sillimanite-biotite schist of the St. Regis Formation (7756, from Moscow Bar Ridge); (f) Garnet-muscovite-biotite schist of the Wallace Formation (7726, from upper Skull Creek); (g) Banded phlogopite gneiss and diopside gneiss of the Wallace Formation (7708, from the junction of Collins and Skull Creeks); (h) Scapolite-biotite-diopside gneiss of the Wallace Formation (7806, from Bald Knob). The scale in millimeters on *g* applies to all the photomicrographs. Plane polarized light unless specified otherwise. SC = scapolite; S = sillimanite; M = muscovite; D = diopside; P = phlogopite; B = biotite; G = almandine garnet; Q = quartz; O = oligoclase.

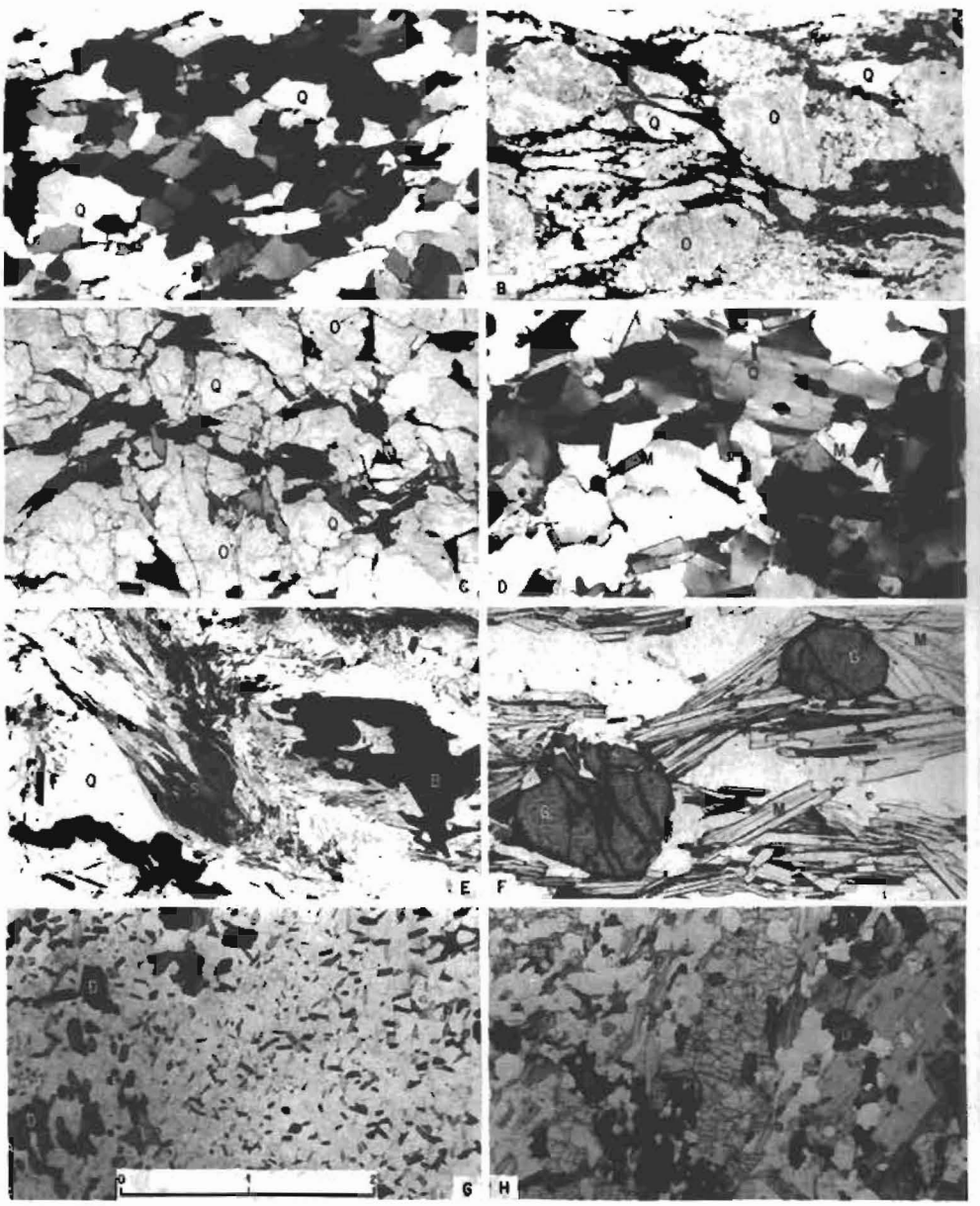

Fig 4

C.S. HUTCHISON Fi

Figure 4

The strongly developed F_1 isoclinal folding, combined with a nearly perfect axial plane schistosity and shearing, has caused the intercalation in other formations near the contacts and within the formation outcrop. Thus, near the Idaho batholith, along the main North Fork of the Clearwater River (Figure 3), 2- to 12-meters-thick layers of banded tremolite-diopside-biotite-oligoclase-quartz calc-silicate are intercalated in the metaquartzite. It is uncertain if these calcareous rocks, which are structurally conformable, are part of the Burke Formation or have been sheared in along fault planes that parallel the F_1 schistosity.

Near Mush Point (Figure 3), the metaquartzite contains muscovite or muscovite and biotite. A crudely foliated, dark brown to black gneiss at Mush Point contains garnet, sillimanite, biotite, muscovite, and quartz. In thin section, the garnet and sillimanite are strongly shimmered with muscovite, probably as a result of closeness to the Idaho batholith.

REVETT FORMATION

In one report Hietanen (1968) described the Revett Formation as 180 meters of coarse-grained, white, thick-bedded quartzite, and in a previous report (Hietanen, 1967) as 200 to 500 meters of thick, coarse-grained pure quartzite with muscovite laminae separating the individual beds. The total thickness was estimated by Ross (1970) at 366 meters.

The characteristic rock is a white, thick-bedded metaquartzite composed of at least 95 percent sutured quartz of 0.5 to 3 millimeters in grain size. Minor amounts of muscovite, oligoclase, and biotite are the components. Some layers of banded, black and gray speckled, foliated biotite-oligoclase-quartz gneiss, with individual bands of 1 to 2 centimeters in thickness, are interlayered with the thick metaquartzite beds (Figure 4c).

There are also a few thin sillimanite-garnet-quartz-muscovite-biotite-oligoclase schist layers, and some metaquartzite beds contain minor epidotes. Some gneisses contain a little tremolite. It is uncertain if these calc-silicate-bearing rocks are strictly part of the Revett Formation, or if they have been interfoliated conformably or sheared in from the Wallace Formation. The formation shown in Figure 3 is predominantly a thick-bedded muscovite-bearing metaquartzite. Unlike the metaquartzite ascribed to the Burke Formation, this metaquartzite is generally free of cataclasis.

ST. REGIS FORMATION

Hietanen (1967) described the St. Regis Formation as 100 to 300 meters of garnet-mica schist with some layers of biotite gneiss or biotite quartzite, and in another report (Hietanen, 1968) as 100 meters of garnet-mica schist. Ross (1970) estimated the range of thickness to be from 300 to 2,200 meters. To the south, the Ravalli Group, including the Burke, Revett, and St. Regis Formations, have been estimated by Reid and others (1973) at 1,520 meters thick.

The characteristic rock is a quartz-oligoclase gneiss with closely spaced foliae of biotite and muscovite schist (Figure 5). Many of the quartz-feldspar layers are as thick as 3 centimeters, but most are less. Shear or cataclastic layers are quite commonly parallel to the foliation, which is planar in most places, but in some localities well-developed crenulations or chevron folds (Figure 4e) are present. Some feldspathic layers contain microcline or untwinned alkali feldspar. The muscovite is of the 2M1 type (Powder Data File, 1974). In the thicker schist layers, sillimanite and garnet occur in addition to the universally present muscovite and biotite (Figure 4).

Figure 5. Hand-specimen appearance: (a) Foliated quartzo-feldspathic band in mica-feldspar gneiss of the St. Regis Formation (7604, from upper Quartz Creek); (b) Fold in banded phlogopite and calc-silicate gneiss of the Wallace Formation (7744, from upper Quartz Creek); (c) Banded phlogopite-rich and calc-silicate layers in the Wallace Formation (7729, from upper Quartz Creek); (d) Quartzo-feldspathic veining in foliated amphibolite (7599, from upper Quartz Creek); (e) Mica schist and concordant pegmatite veining of the St. Regis Formation (7585, from lower Quartz Creek); (f) Banded metaquartzite, green calc-silicate, and phlogopite gneiss of the Wallace Formation (7784, from Indian Henry Ridge); (g) Porphyritic rhyodacite sill (7587, from lower Quartz Creek); (h) Quartz monzonite of the Idaho batholith (7655, from North Fork of the Clearwater River, southwest corner of map); (i) Strongly porphyritic rhyodacite dike or sill (7800, from Mush Point); (j) Weakly porphyritic rhyodacite sill (7768, from lower Skull Creek); (k) Granodioritic pegmatite in the Wallace Formation (7780, from Bald Knob). The scale for each specimen is given in centimeters. Specimen numbers are those of the geology department at the University of Malaya.

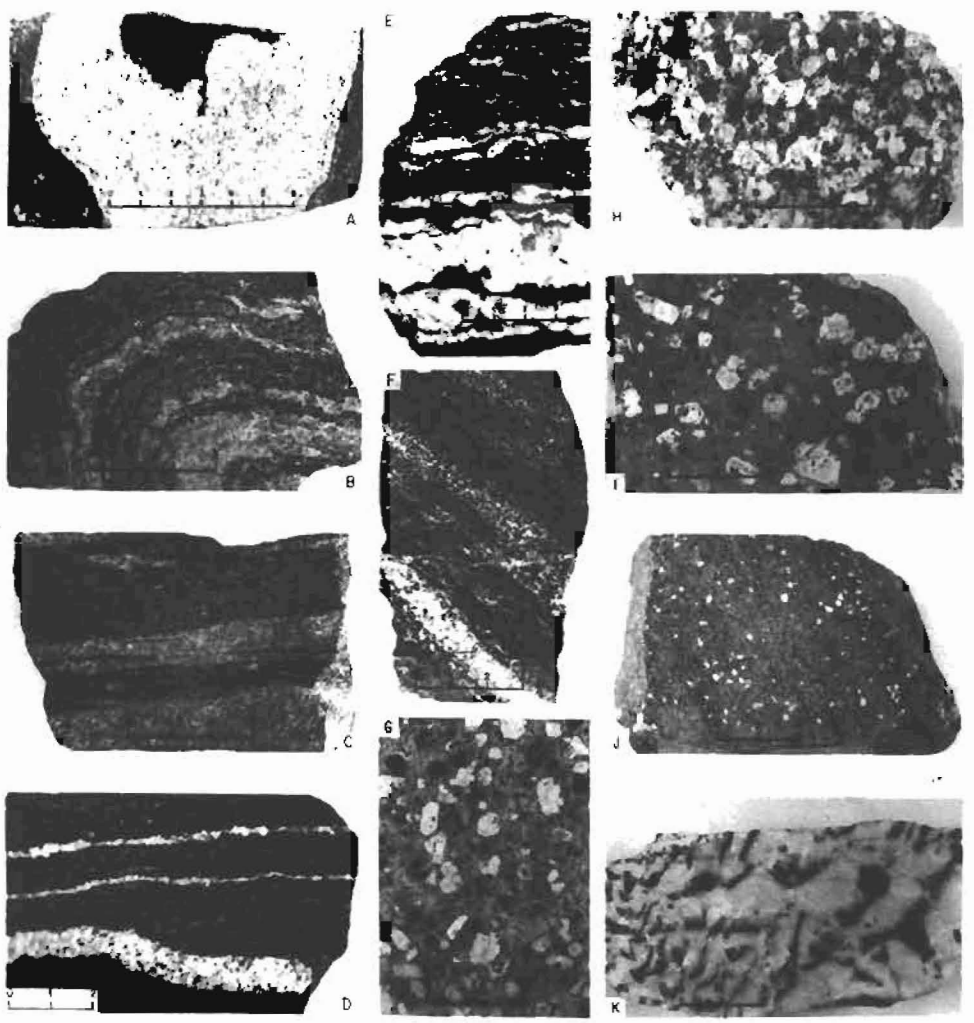

Figure 5

In upper Quartz Creek near the junction with Cougar Creek (Figure 3), the thicker layers of fine-grained muscovite metaquartzite contain small amounts of oligoclase and biotite about 1 millimeter in grain size (Figure 4). It is uncertain if this metaquartzite is part of the St. Regis Formation or is infolded metaquartzite of the Revett Formation. Likewise, there are areas of diopside-plagioclase-phlogopite gneiss at the junction of Quartz Creek with the main North Fork of the Clearwater River. These may be infolded or sheared-in gneiss of the Wallace Formation. The strong isoclinal F_1 folding and shearing parallel to the axial plane schistosity (Figure 6) can be expected to repeat parts of one formation within the major outcrop of another. The absence of marker horizons makes it impossible to map all these infolds separately.

WALLACE FORMATION

The Wallace Formation was subdivided by Hietanen (1967) into three units: the lower gneiss, the lower schist, and the upper gneiss. Descriptions of the three units are given below.

Wallace Lower Gneiss

The lower unit of the Wallace Formation, described by Hietanen (1967) as the "lower quartzite gneiss," is composed of 200 to 1,900 meters of white granular quartzite overlain to the south by interbedded diopside and biotite gneiss and to the north by interbedded biotite quartzite, biotite granofels, and phlogopite-bearing carbonate granofels. The diopside gneiss, biotite granofels, and carbonate granofels contain scapolite (Hietanen, 1967). Hietanen (1968) described the lower gneiss as a 100-meter-thick, white granular quartzite overlain by more than 300 meters of thin-bedded biotite quartzite.

The thickness of the Wallace Formation was estimated at 1,200 to 1,830 meters by Ross (1970). However, Reid and others (1973) estimated 3,050 meters for the lower gneiss and the same for the upper Wallace. These widely diverging estimates in thickness must reflect the difficulty of accurate measurement in complexly folded terrane that is characterized by the absence of distinctive marker beds.

The common and typical rock assemblage is distinctive, so that the contact with the underlying St. Regis Formation can be accurately mapped (Figure 3). The formation is composed of well-bedded rhythmic repetitions of 1- to 4-centimeters-thick beds of white saccharoidal metaquartzite (grain size 0.2 millimeter) interbedded with phlogopite-rich and calc-silicate layers. The layers alternate rapidly in color from pure white to speckled brown or black (colored by phlogopite) to pale green (colored by calc-silicates, Figure 5). In some places the metaquartzite layers weather pale brown and may be very friable.

Most of the white metaquartzite layers are composed of granular quartz and oligoclase of 0.2 millimeter grain size. The speckled layers are caused by phlogopite flakes that are randomly oriented in a matrix of quartz and oligoclase (Figure 4). Other layers are rich in slightly larger porphyroblasts of diopside and tremolite about 1 millimeter in size. Some layers are calcite rich. Accessory minerals are sphene and zircon.

Scapolite of mizzonite composition occurs in a few places and is not restricted to the top of the formation as suggested by Hietanen (1968). It occurs as large porphyroblasts in rocks exposed in Quartz Creek, near the contact with the St. Regis Formation. It also occurs in higher units in rocks that crop out in Skull Creek (Figure 4). Its

Figure 6. Details of outcrops: (a) Pegmatite sill and dike complex in the St. Regis Formation along lower Skull Creek. The pegmatite sill changes to a dike and anastomoses somewhat. The St. Regis Formation is composed of interlayered mica schist and quartzo-feldspathic gneiss. (Kodachrome 2291). (b) Tight F_1 isoclinal folds in the garnet-quartz-mica schist and quartzo-feldspathic gneiss sequence of the St. Regis Formation of lower Skull Creek. The schistosity passes through the sharp fold noses to give an axial plane schistosity. (Kodachrome 2306). (c) Similar small-scale F_2 folds in quartz-mica schist and quartzo-feldspathic gneiss of the steeply dipping St. Regis Formation at the junction of Cougar and Quartz Creeks. The parallel injection of pegmatite along the foliation and the incipient migmatization of the whole rock is apparent. (Kodachrome 2292). (d) Complicated ptygmatic folding of quartzo-feldspathic layers and pegmatitic veins in vertically foliated quartz-mica schist of the St. Regis Formation. Locality: North Fork of the Clearwater River, south of Quartz Creek. (Kodachrome 2301).

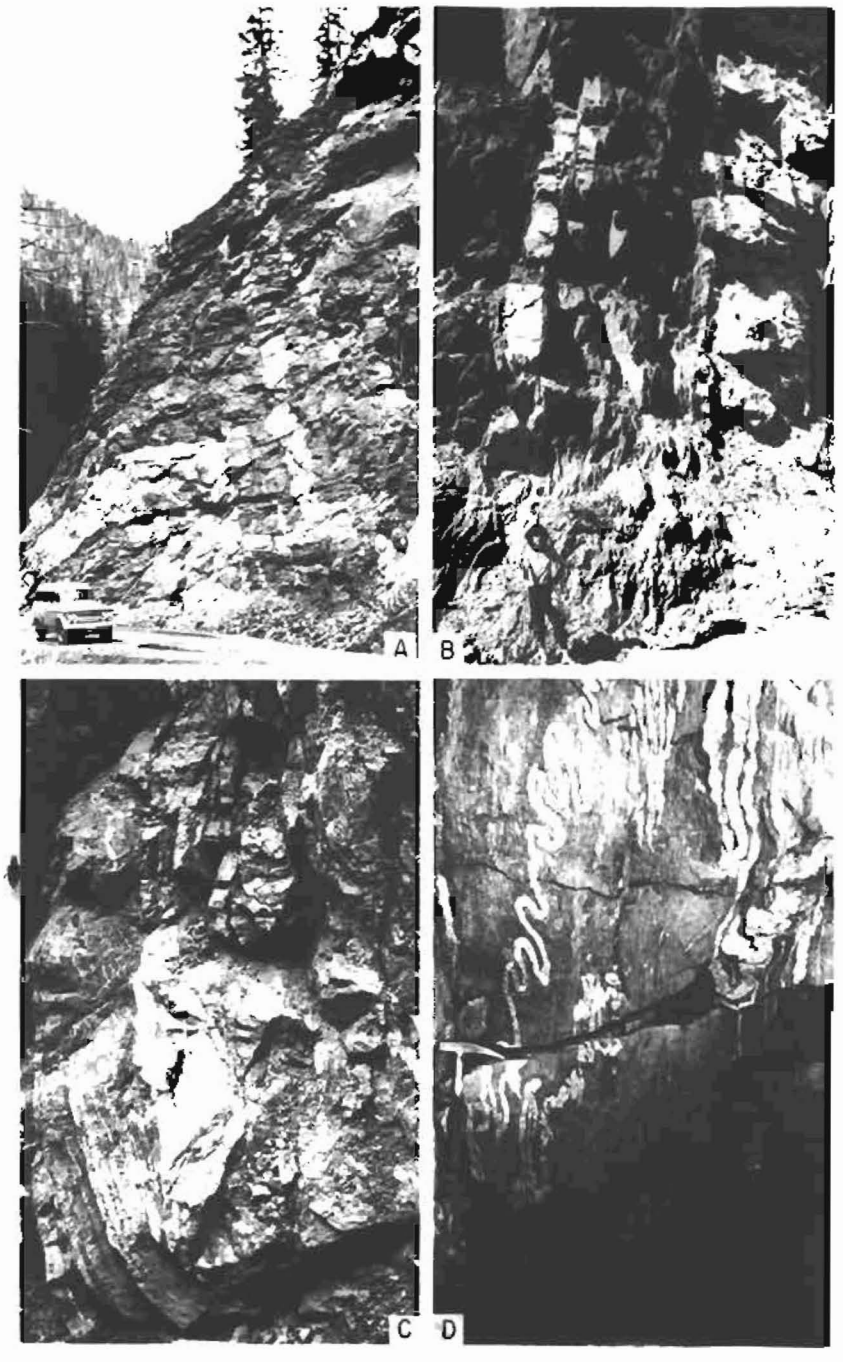

C. S. HUTCHISON Fig 6

Figure 6

occurrences are not related to the outcrop of the Idaho batholith. The presence of scapolite possibly resulted from the F_1 metamorphism of halite beds within the formation (Hietanen, 1967), and not as a product of metasomatism from the granite.

Occasionally there are much thicker beds of granular white quartz-oligoclase meta-arenite, but the common assemblage is a rapid rhythmic interbedding on a centimeter scale. Folding and recrystallization have caused the contacts between the individual beds to be diffused and in many places pulled into boudins and lenses (Figure 7); some beds are discontinuous (Figure 5c).

Wallace Lower Schist

Hietanen (1967) described the lower schist as a 200- to 300-meter-thick garnet-mica schist, generally with other aluminum silicates. Outcrops on upper Skull Creek and Wallow Mountain (Figure 3) show it to be composed of a well-foliated muscovite-biotite-garnet-quartz schist containing some sillimanite (Figure 4). Feldspar is rare or absent. The grain size is from 1 to 2 millimeters.

Wallace Upper Gneiss

The Wallace upper gneiss is identical to the lower gneiss. It is thin bedded and characterized by a rhythmic alternation of white saccharoidal meta-arenite that contains phlogopite-rich layers and green calc-silicate layers composed of calcite, diopside, and tremolite. Hietanen (1967) gave its thickness as 200 meters and described it as composed of mainly diopside-plagioclase gneiss and some biotite gneiss.

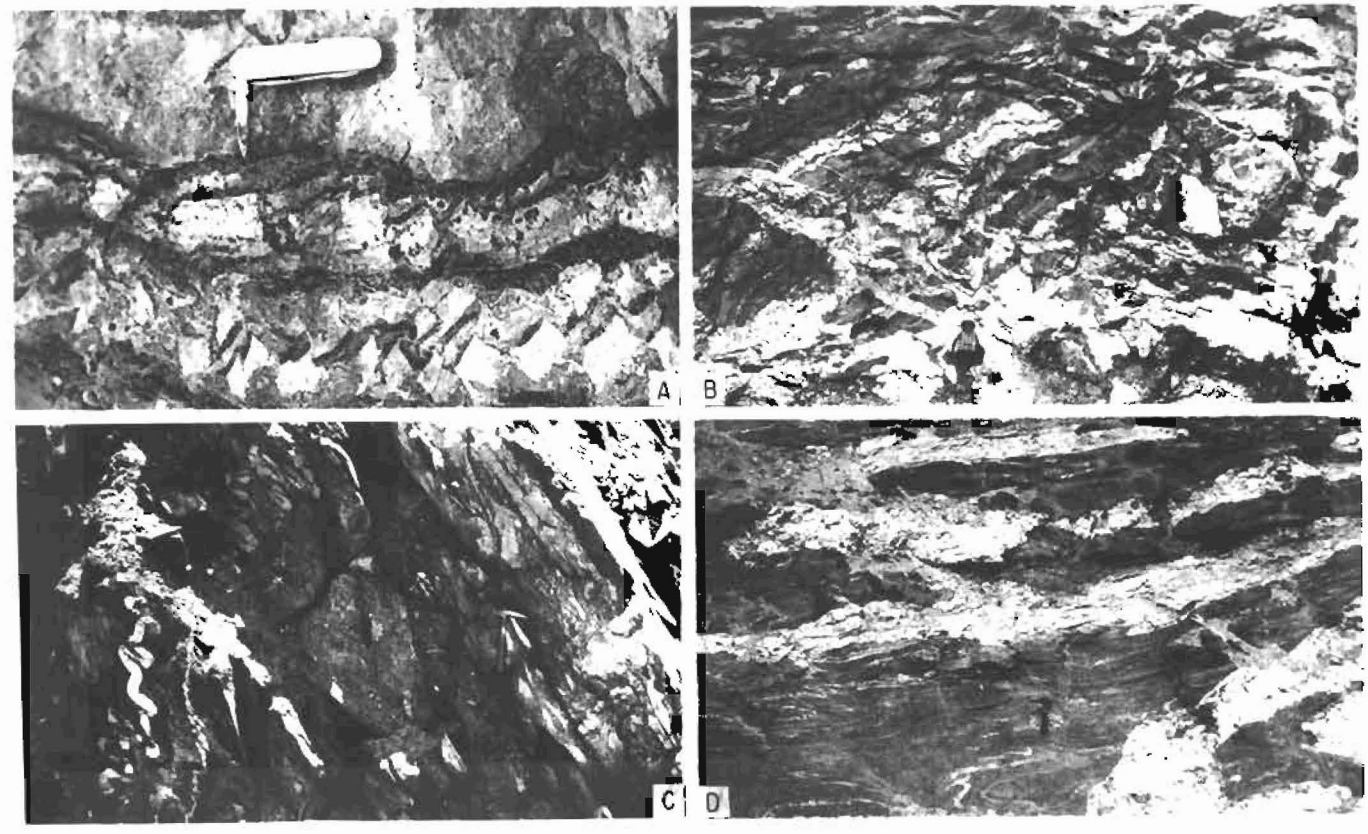

Figure 7. Details of outcrops: (a) Boudinage of white metaquartzite beds within green calc-silicate and dark phlogopitic gneiss of the Wallace Formation. Locality: Wallow Mountain. (Kodachrome 2334). (b) Strongly migmatized St. Regis Formation, 1/4 mile up Quartz Creek. The schist and gneiss are pervaded by pegmatite, predominantly parallel but also at high angles to the schistosity. (Kodachrome 2337). (c) Complex boudinage of intricate ptygmatic folds in mica schist of the St. Regis Formation. Locality: Pear Creek. (Kodachrome 2328). (d) Pegmatite pervading the mica schist of the St. Regis Formation on Cougar Creek. (Kodachrome 2321).

INTRUSIVE ROCKS

FOLIATED AMPHIBOLITE SHEETS (PURCELL SILLS?)

Conformable sheets of amphibolite occur in all the metasedimentary formations with which they share the same F_1 schistosity (Figure 3). Their fabric is entirely dynamothermal metamorphic with no igneous relicts; fining of the grain size towards the contacts, had it originally existed, has not been preserved. The sills range in thickness from 1 to 5 meters. Occasionally swarms of several thin sheets occur in close proximity. They locally cut across the foliation of the metasediments; otherwise, the sheets are remarkably conformable. The amphibolite is composed of abundant hornblende and andesine with accessory sphene and quartz. A common grain size is 1 to 2 millimeters. In outcrop the rock is well-lineated and black to dark green with white feldspar specks (Figure 5). The foliation parallel to the F_1 schistosity of the country rocks is accentuated by some segregation of the hornblende and plagioclase into imperfect layers. Some specimens have coarser feldspathic layers and occasional cataclastic zones. The sphene may be replaced by anatase in some places. A few specimens contain red garnet porphyroblasts up to 10 millimeters in diameter (Figure 8).

The amphibolite sheets are not resistant to erosion, for in common with all rocks of the Clearwater National Forest, the mechanical disintegration of fresh exposures into a gravel scree is extremely rapid. Hietanen (1963, 1968) says little of the amphibolites and generally has not noticed that they form conformable sheets. The amphibolites correlate well with what Reid and Greenwood (1968) called the Type I amphibolites, with an emplacement age of about 1,200 m.y. (Bishop, 1973).

IDAHO BATHOLITH GRANITOIDS

Good exposures of the northern contact of the Cretaceous Idaho batholith occur along the North Fork of the Clearwater River (Figure 3; Figure 9). The batholith rocks appear nonporphyritic in outcrop, but studies of thin sections and polished slabs show them to be weakly porphyritic and from 0.2 to 4 millimeters in grain size (Figure 5). The common rock is pale gray to cream, weathering to slightly brownish. The major rock is a hornblende-biotite-quartz monzonite containing orthoclase microperthite, oligoclase, euhedral hornblende (pleochroic from yellow through green to brown), biotite, and quartz (Figure 8).

The texture is characteristically hypersolvus, as described by Tuttle and Bowen (1958), in which the plagioclase is mostly exsolved from perthite. Using the methods of Goldsmith and Laves (1954) and Wright (1968), the alkali feldspar was determined to be predominantly orthoclase of zero triclinicity with normal cell dimensions, and its potassium-rich phase has a composition range from Or_{85} to Or_{100}. Farther from the contact, the alkali feldspar was determined to be intermediate microcline, showing no lamellae but only carlsbad twinning, of cell parameters similar to SH 1070 and Spencer B of Wright (1968).

Some cataclastic zones have augen of oligoclase and alkali feldspar and concentrations of epidote and tremolite along the shear planes. Pink porphyry dikes of grain size ranging from 0.05 to 2.5 millimeters, containing phenocrysts of quartz, orthoclase, oligoclase, and biotite, occur in the outer zones of the batholith (Figure 5). The contact between the Bungalow stock (43.1 $\pm$ 1.4 m.y.; Hietanen, 1969) and the older batholithic rocks is just south of the present study area. The pink dikes may be related to this granite of Tertiary age.

Figure 8. Thin-section appearance: (a) Rhyodacite sill (7605, cross-polars, from upper Quartz Creek); (b) Foliated garnet amphibolite sheet (7691, from the junction of Nub and Skull Creeks); (c) Rhyodacite sill (7689, from junction of Pear and Skull Creeks); (d) Diabase sill (7579, from junction of Quartz Creek and North Fork of the Clearwater River); (e) Rhyodacite sill (cross-polars) showing variolitic matrix; (f) Hornblende-plagioclase diabase (7634, cross-polars, from the North Fork of the Clearwater River, southwest corner of map); (g) Orthoclase-quartz monzonite of the Idaho batholith (7655, cross-polars, from North Fork of the Clearwater River, southwest corner of map); (h) Microcline granodiorite orthogneiss in the Wallace Formation (7709, cross-polars, from junction of Collins and Skull Creeks). The scale in millimeters on *d* applies to all the photomicrographs. Plane polarized light used throughout unless otherwise specified. OR = orthoclase microperthite; MI = microcline; B = biotite; Q = quartz; G = garnet; H = hornblende.

8

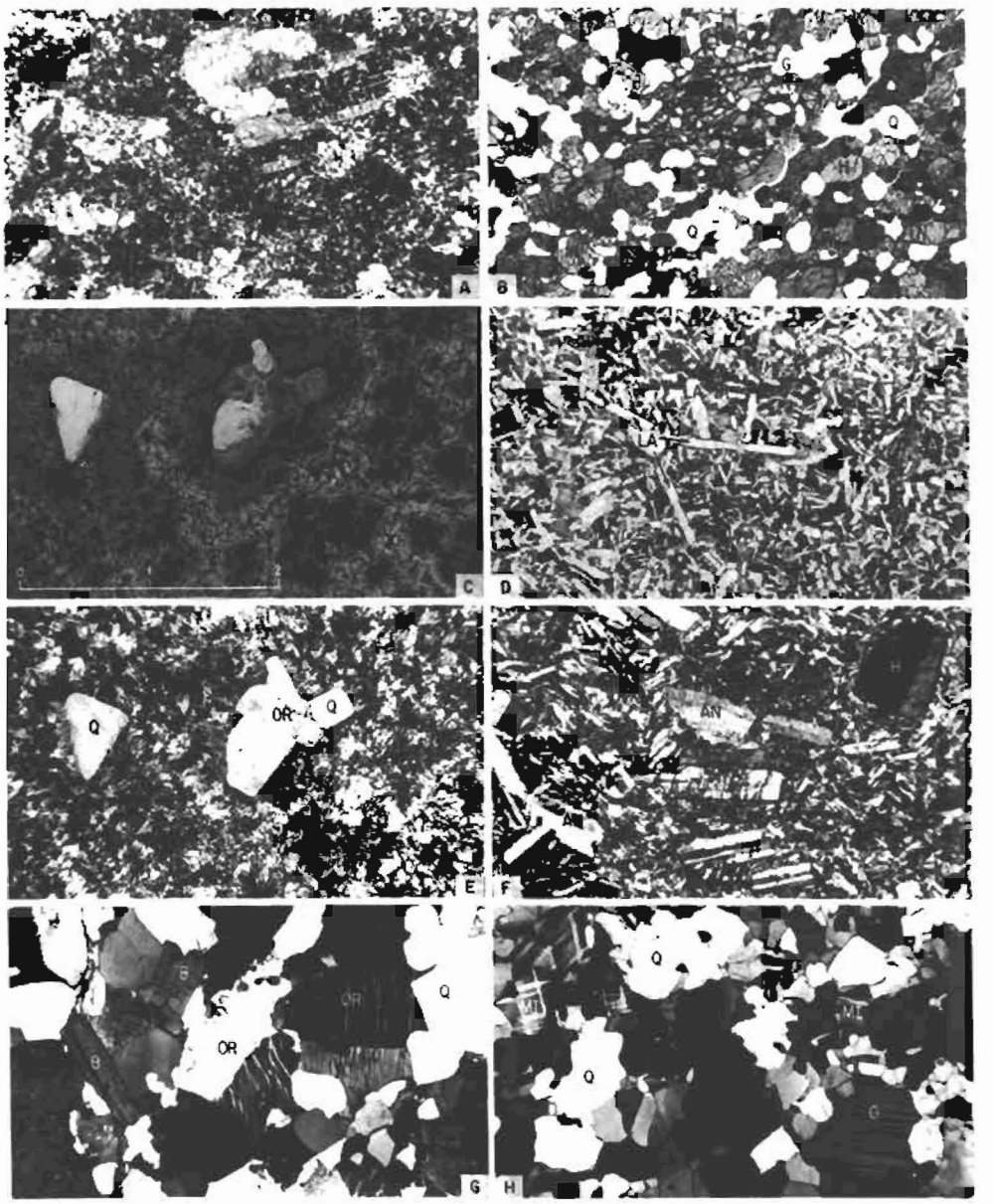

C.S. HUTCHISON Fig 8.

Figure 8

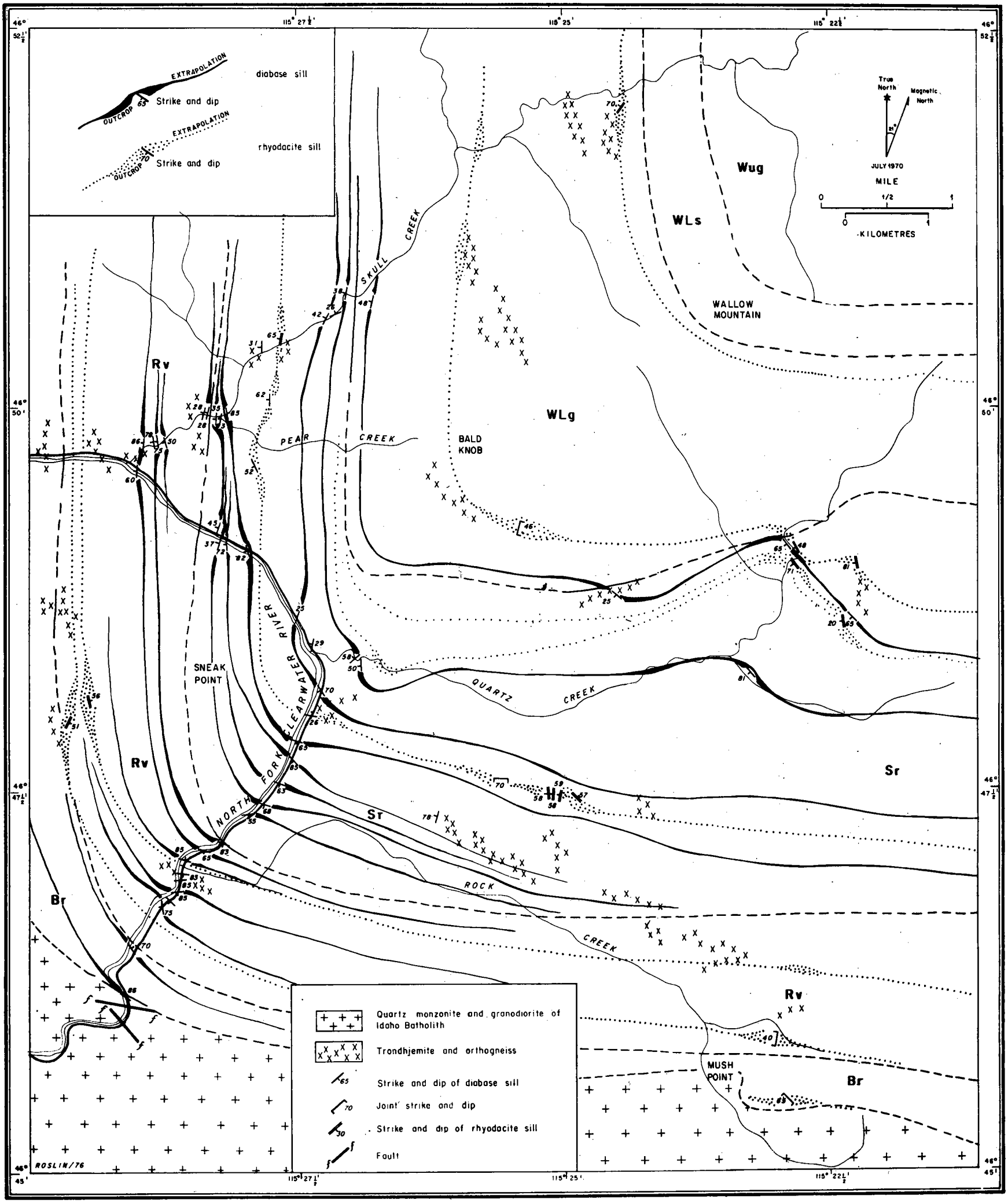

Figure 9. Outline geologic map of the same area as Figure 3, showing the outcrops of diabase and rhyodacite sills.

PEGMATITES

Pegmatites of grain size ranging from 5 millimeters to 10 centimeters occur within all the metamorphic country rocks, including the amphibolite sheets. Many are crudely tabular to veinlike and from 1 centimeter to many tens of meters thick (Figure 6). On a bigger scale, large volumes of metasediments may be engulfed by pegmatite to form migmatite (Figure 7). The pegmatite bodies are normally 1 to 3 meters wide and roughly conformable with the F_1 schistosity of the metasediments (Figure 5), but here and there they are discordant. Most of the pegmatites are folded together with the country rocks, are boudinaged, and may be ptygmatically folded (Figure 6).

There are two distinct types, which may be related to two major periods of intrusion in the Cretaceous and Tertiary or to several different phases within the Cretaceous batholith. One type is dominated by coarsely perthitic, near maximum microcline, as determined by the method of Stewart (1975). The potassium-rich phase is richer in orthoclase than 85 percent. The other type is dominated by cryptoperisteritic oligoclase of composition about Ab_{88} with low temperature X-ray characteristics. This type contains only a small amount of microcline. The oligoclase pegmatites are white in hand specimen, while the microcline pegmatites are pink. Graphic texture is common in both (Figure 5).

In addition to feldspar, quartz is present. Mafic minerals make up only a small proportion. Muscovite of type 2M1 is universally present and is more abundant than biotite. The biotite has crystallized in shear and cataclastic zones within the pegmatite, so that unlike the muscovite, it shows a distinct preferred orientation. Small euhedral, limonitized garnet crystals are quite common. Myrmekite is occasionally present.

Hietanen (1963) noted the two pegmatite types. She felt that they were related to the Idaho batholith, but she could not reconcile the existence of orthoclase in the batholith and maximum microcline in the pegmatites. The alkali feldspars in the pegmatites are coarsely perthitic, while in the batholith they are cryptoperthitic. It is important to realize that factors other than cooling rates may be important in determining the structural state and exsolution of the alkali feldspars. The availability of water in the outer zones of the crystallizing batholith was obviously less than in the pegmatite veins and the crystallizing metasediments in which they occur. The pegmatite fluid undoubtedly also contained more water than the batholith magma. Water does not increase the diffusivities of the alkalis; however, it may be involved if it provides an alternative to the solid-state order-disorder and exsolution reaction (Yund, 1975). Therefore, some of the microstructural changes may involve local dissolution and reprecipitation of the feldspar. Alternatively, deformation may influence the nature of the final microstructure either by affecting the rate or by changing the process. The pegmatites and their metamorphic envelope were obviously subjected to considerably more deformation than the batholith during their crystallization histories. Therefore, these differences in feldspar details between pegmatites and batholith may be reconciled.

DIABASE SILLS

Aphanitic black to dark gray diabase sills have a common thickness of 30 centimeters but range from 15 to 50 centimeters. Each sill is remarkably regular in thickness, but bifurcations have been seen. The sills are more resistant to weathering than the metasediments and amphibolites

and form subdued linear ridges on the mountainsides, which occasionally can be seen on air photographs. They are intruded conformably along, but occasionally slightly cross-cut, the F_1 schistosity of the metasediments (Figure 9). They are intruded into cold country rocks and display well-defined chilled margins, which are glassy in some places and occasionally contain schist xenoliths.

Texturally the sills are very fine grained, cryptocrystalline, or even glassy. They contain abundant plagioclase phenocrysts up to 2 millimeters long. The average groundmass is less than 0.1 millimeter, but it is in many places recrystallized to a coarser grain (Figure 8). The thicker sills have coarser-grained interiors characterized by an ophitic intergrowth of plagioclase and augite (Figure 8). The deuteric crystallization is variable. Some sills show little alteration, and the phenocrysts in these sills are composed of andesine-labradorite An_{42} to An_{56} and diopside to subcalcic augite (2V 40 to 65°). A few contain euhedral basaltic hornblende crystals. The common accessory minerals are iron and titanium oxides and anatase. The igneous flow is occasionally preserved as lineated plagioclase laths.

Most of the pyroxene is completely replaced or remains only as a few relicts. It is commonly replaced by actinolite, hornblende, or chlorite. In some places the plagioclase is replaced by oligoclase to albite and may be saussuritized. The groundmass is recrystallized to an intergrowth of sericite, green biotite, and feldspar and some epidote and calcite. Devitrification has resulted in small spherulitic aggregates of radiating amphibole needles and feldspar. In the analogous Coeur d'Alene district, the recrystallized sills have been referred to as lamprophyres, and they have been shown to grade into unrecrystallized diabase (Hobbs and Fryklund, 1968).

The sills were clearly emplaced after the major shearing of the country rocks, for they retain their igneous texture and chilled margins and have a complete lack of metamorphic foliation. In the area of study only one sill outcrop was observed to show cataclasis. These features together indicate their young age, which is probably Eocene.

PORPHYRITIC RHYODACITE SILLS

The pale gray sills contain white and pink phenocrysts and range from 20 centimeters to 5 meters in thickness (Figure 9). Most are strongly porphyritic, but some varieties are weakly porphyritic (Figure 5). The groundmass has a grain size of 0.1 to 0.2 millimeter, and phenocrysts may range up to 8 millimeters. Where the sills display a distinct chilled margin against the metasediments, the grain size is only 0.06 millimeter.

The phenocrysts are composed of oligoclase to andesine An_{22} to An_{34} but are more commonly in the oligoclase range. All are sericitized. Orthoclase showing carlsbad twinning and a complete absence of polysynthetic twinning is also common. The orthoclase:plagioclase ratio varies, so that some varieties are dacitic, but most are rhyodacitic. Quartz is euhedral bipyramidal. Pseudomorphs of chlorite after biotite are also common as phenocrysts.

The groundmass appears as if it were originally glassy, but it has devitrified, in most places variolitically (Figure 8). The spherules are commonly 1 millimeter in diameter and consist of a fine intergrowth of quartz and feldspar. The rest of the groundmass is a fine-grained intergrowth of sericite, chlorite, green-yellow amphibole, plagioclase, epidote, and calcite (Figure 8).

The sills have an igneous texture and have not been foliated or sheared. They are, therefore, considered to be genetically related to igneous activity of Eocene age. Similar dikes are described in the Coeur d'Alene district (Hobbs and Fryklund, 1968) and are widespread throughout the rest of the Idaho batholith. There is no field evidence to suggest a relative age in comparison with the diabase sills, since the rhyodacite sills occur separately from the diabase sills.

ORTHOGNEISS

There are numerous outcrops of a distinctive white, leucocratic, even-grained tonalitic to granodioritic orthogneiss (Figure 9) in the Wallace Formation, especially in Skull Creek and around Bald Knob. Grain size ranges from 1 to 2 millimeters, and the rocks are remarkably even grained and locally may be crudely foliated (Figure 8). The relationship to the Wallace Formation metasediments is not known with certainty, for fresh outcrops are scarce. However, the orthogneiss masses are largely conformable with the bedding of the country rocks. The mineralogy in decreasing order of abundance is oligoclase, quartz, biotite, microcline, and muscovite. Mafic minerals make up only 1 to 2 percent of the rock.

These rocks may possibly correlate with one of the many orthogneisses described by Reid and others (1973) from the Clearwater Orogenic Zone, many of which outcrop within the Wallace Formation, or they may correlate with the orthogneiss dated at 82 m.y. by Chase and others (1978). The orthogneiss may also correlate with the late stage Idaho batholith leucocratic rocks in the Atlanta lobe of the batholith as described by Swanberg and Blackwell (1973).

GEOCHEMISTRY

A selection of rocks was analyzed by the method of Norrish and Hutton (1969) as modified by Hutchison (1974, 1975a). The iron oxide analyses were standardized to an arbitrary $FeO/(FeO + Fe_2O_3)$ ratio of 0.75. Barth mesonorms were calculated using a computer program based on Hutchison (1975b). The analyses of a representative selection of metasedimentary rocks are given in Table 1. The absence of normative corundum in the Wallace Formation specimens shows that the sediments were not particularly aluminous.

Chemical analyses and Barth mesonorms of selected amphibolites and pegmatites are given in Table 2. The amphibolites are all low in potassium and are constant chemically except for the garnetiferous specimen. All have abundant normative actinolite, while the garnetiferous specimen is strongly hypersthene normative, indicating that the formation of garnet was controlled by the bulk chemistry. The pegmatites are rich in normative orthoclase and albite.

Chemical analyses and Barth mesonorms of a selection of diabase sills are given in Table 3. There is a range in SiO_2 contents and in the relative amounts of normative biotite and hypersthene.

Chemical analyses and Barth mesonorms of representative granitoids are given in Table 4. It is interesting that all the granitoids, whether of the sills or the orthogneiss associated with the Idaho batholith, have similar characteristics, adding support to the conclusion that they are cogenetic. All are relatively rich in sodium so that no true granite exists, and they lie within the adamellite and granodiorite fields of Streckeisen (1976).

Table 1. Chemical analyses and Barth mesonorms of metamorphic rocks.

OXIDE	7621	7671	7687	7707	7734	7756	7796
SiO_2	69.03	95.76	75.13	70 36	71 08	67.57	62 86
Al_2O_3	15.80	2 59	12.53	8 23	10.72	18.08	19.21
TiO_2	.70	.12	.54	.38	.43	.79	1 03
Fe_2O_3	1 57	.16	71	44	.67	1 20	1 94
FeO	4.72	47	2.14	1 33	2 01	3 59	5 81
MnO	.16	.03	.06	03	06	04	.07
MgO	61	00	45	3.98	3.38	1.71	1 07
CaO	.50	04	2.08	8.04	7 60	34	07
Na_2O	1 16	.00	3 53	3 67	1 97	1.34	.00
K_2O	3 13	69	2.31	1.01	2 72	4 46	3.74
P_2O_5	.11	.00	.14	07	.11	.04	.01
SO_3	00	.00	02	08	.00	12	.00
Ign. Loss	2 09	43	.19	3.99	40	1 89	3.56
Less O for S			01	05		.07	
Total	99 58	100.29	99.82	101.58	101 15	101 10	99 37
	Barth Mesonorms of the rocks						
Qtz.	49 32	92 74	39.91	30.89	36.09	40.48	48.93
Cor.	12.23	2 16	1 64			12.43	18 03
Or.	12.72	3.87	10.43		6.07	19.52	15.55
Ab.	11.11		32 43	33.91	17 87	12.40	
An.			7.70	3.03	12.51		
Salic	85.38	98.77	92.11	67.83	72.54	84.84	82.50
Act.				8.39			
Biot.	11.21	.83	5 65	10.02	16 27	12 22	13 64
Wo				12.24	9.34		
Hgte.	1.75	.18	.76	.47	.71	1.29	2 21
Ilm.	.29	.09				55	1 44
Sph.	1.13	.13	1.15	82	.91	.88	.18
Apte	.25		.30	.15	.23	09	.02
Pyr.			.03	.08		.13	
Femic	14.62	1.23	7.89	32.17	27.46	15.16	17.50
Mg/Fe	21/79	0/100	30/70	86/14	77/23	53/47	31/69
Plag.	Ab_{100}		Ab_{81}	Ab_{92}	Ab_{59}	Ab_{100}	

* $Fe_2O_3/(FeO + Fe_2O_3)$ calculated as .75 from total iron analysis

7621: St Regis Formation, foliated (garnet)-muscovite-bi tite oligoclase-quartz grey gneiss. 7671 Revett Formation, white massive (biotite)-(garnet)-(oligoclase)-muscovite metaquartzite. 7687: Revett Formation, biotite-oligoclase-quartz foliated banded black and white speckled gneiss with metaquartzite layers. 7707: Wallace Formation, banded white metaquartzite, with dark brown speckled phlogopitic layers, and green calc-silicate layers. Total mineralogy quartz, oligoclase, phlogopite, diopside, tremolite and calcite. 7734 Wallace Formation, banded green calc-silicate and white metaquartzite. Total mineralogy: actinolite, diopside, microcline and quartz. 7756 St Regis Formation, sillimanite-almandine-biotite-muscovite-oligoclase-quartz dark grey cmeyron folded schist. 7796 Burke Formation, sillimanite-garnet-biotite-muscovite-quartz dark brown gneiss

Table 2. Chemical analyses and Barth mesonorms of amphibolite and pegmatite.

OXIDE	7580	7626	7691	7776	7611	7682
SiO_2	49.71	50.35	50.18	50.01	72.42	70.82
Al_2O_3	14.43	14.32	12.56	14.02	15.25	15.63
TiO_2	1.81	1.76	3.51	1.88	.01	.01
Fe_2O_3	3.22	3.48	4.41	3.34	.08	.02
FeO	9.66	10.44	13.23	10.01	.23	.07
MnO	.21	.22	.27	.23	.00	.00
MgO	5.59	5.67	4.57	5.76	.00	.00
CaO	10.85	11.08	8.92	10.43	.25	.05
Na_2O	1.87	1.73	.79	2.16	2.23	1.59
K_2O	70	.70	.59	.75	9.60	11.58
P_2O_5	.08	.22	.41	.17	.02	.02
SO_3	.03	.04	.27	.00	.00	.00
Ign. Loss	.51	.65	.28	.64	.43	.31
Less O for S	.02	.02	.16			
Total	98.66	100.64	99.83	99.40	100.52	100.10
	Barth Mesonorms of the rocks					
Qtz.	3.64	4.21	13.77	2.90	20.69	16.05
Cor.					.87	.49
Or.					56.70	68.79
Ab.	17.55	15.99	7.55	20.12	20.11	14.37
An	30.22	30.11	30.85	27.33	1.08	08
Salic	51.40	50.30	52.17	50.35	99.45	99.79
Act.	28.36	28.05	.59	27.61		
Biot.	6.91	6.81	5.94	7.35	.40	.13
Hyp.	5.66	6.78	27.38	6.62		
Mgte.	3.52	3.74	4.91	3.62	.08	.02
Sph.	3.95	3.79	7.81	4.08	.02	.02
Apte.	.17	47	.91	.37	.04	.04
Pyr.	.03	.05	.30			
Femic	48.60	49.70	47.83	49.65	.55	.21
Mg/Fe	54/46	53/47	42/58	54/46	0/100	0/100
Plag.	Ab_{37}	Ab_{35}	Ab_{20}	Ab_{42}	Ab_{95}	Ab_{99}

7580: amphibolite containing dark green hornblende, labradorite, minor quartz and accessory sphene. 7626: foliated amphibolite containing abundant green-brown hornblende and andesine, with accessory quartz and anatase. 7691: amphibolite with green-brown hornblende, sieve porphyroblasts of garnet, quartz, opaque minerals and rare plagioclase. 7776: foliated amphibolite with abundant green-brown hornblende, andesine An_{45}, minor sphene, chlorite and quartz. 7611: coarse pegmatite containing pink microcline (maximum triclinicity), quartz, oligoclase, muscovite and green biotite. 7682: graphic pegmatite containing microcline, quartz and muscovite.

Table 3. Chemical analyses and Barth mesonorms of diabase sill rocks.

OXIDE	7579	7606	7619	7675	7752
SiO_2	51.78	51.11	51 27	60.57	54.65
Al_2O_3	16 82	14 48	17.34	16.45	14.39
TiO_2	.91	.85	1.64	.96	.73
Fe_2O_3	1.92	2.22	2.33	1.32	1.59
FeO	5 75	6.65	6.99	3.95	4.78
MnO	.12	.16	.16	.09	.11
MgO	6.20	9.02	5.27	2.79	7.73
CaO	8.60	7 70	8.32	4.70	6.75
Na_2O	1.46	2 18	1.91	3.35	1.60
K_2O	.96	1.85	1.69	3.01	1.82
P_2O_5	.15	.28	.37	.30	.23
SO_3	.32	.00	39	.00	.00
Ign. Loss	3.69	2.50	2.92	1.41	5.00
Less O for S	.19		.23		
Total	98.49	99.00	100.37	98.90	99.38
	Barth Mesonorms of the rocks				
Qtz.	12.69	5.77	11.36	20.09	17.05
Cor.			.25	1.21	
Or.				7.12	
Ab	13.94	20.18	17.82	30.98	15 23
An.	38.83	25.02	34 44	18.55	28.32
Salic	65.46	50.98	63.87	77.96	60.61
Act.	3.20	14.15			4 35
Biot.	9.65	18.03	16.60	17.91	18.24
Hyp.	16.84	12.01	12.21		12.91
Mgte	2.13	2.39	2.53	1.42	1.76
Sph.	2.02	1.83	3.56	2.07	1.62
Apte.	33	.60	.80	.65	.51
Pyr.	.36		.43		
Femic	34.54	49.02	36.13	22.04	39.39
Mg/Fe	69/31	73/27	61/39	59/41	77/23
Plag.	Ab_{26}	Ab_{45}	Ab_{34}	Ab_{63}	Ab_{35}

* Iron calculated as in Table 1

7579 contains phenocrysts of labradorite and diopsidic augite in a cryptocrystalline matrix. 7606: contains phenocrysts of augite, hornblende and oligoclase in a fine-grained matrix of chlorite, epidote, plagioclase, opaque minerals, and some quartz. 7619: contains phenocrysts of labradorite, and relicts of augite in a matrix of calcite, sericite, amphibole, and opaque minerals. 7675: The coarse grained centre of a sill. It has a trachytic texture and is composed of andesine and hornblende, with interstitial chlorite, epidote and quartz. 7752: contains phenocrysts of sericitized and calcitized oligoclase in a matrix of chlorite, calcite, actinolite, quartz

Table 4. Chemical analyses and Barth mesonorms of granitoid rocks.

OXIDE	7587	7647	7652	7655	7700	7768	7785
SiO_2	76.71	69.33	75.51	72.88	72 53	70 96	74 40
Al_2O_3	11 65	15 11	12.96	13.59	16.08	15.52	14.56
TiO_2	11	.46	.09	.21	.07	21	04
Fe_2O_3	.28	.77	30	42	.15	.45	11
FeO	84	2.32	.91	1.27	45	1.35	.33
MnO	.02	.05	.02	.03	.04	04	.01
MgO	61	.36	.36	29	35	.62	.31
CaO	.44	1.66	.46	80	1.46	1 68	75
Na_2O	3.70	4.27	3.85	3.85	6.09	4.46	4.55
K_2O	4.68	5.08	5.15	5 59	2.85	3.67	5 05
P_2O_5	01	.10	.00	.02	.03	.09	03
SO_3	.00	00	00	.00	00	.00	.00
Ign. Loss	.87	55	.73	36	.26	.82	44
Total	99.92	100.06	100.33	99 31	100.36	99.87	100.58
	Barth Mesonorms of the rocks						
Qtz.	34.47	20.64	30 41	25 95	21.18	25 96	24.99
Cor		43	38	.07	.52	1 81	.40
Or.	25.77	26.76	28.85	31.39	15 25	18.88	28 60
Ab	33 84	38.61	34.91	35.09	53 86	40.39	40 65
An	1.38	6.02	1.94	3.15	6.70	7.08	3.37
Salic	95.46	92.47	96.50	95.65	97.51	94.12	98.01
Biot.	3.83	5.55	3.00	3 41	2.13	4 78	1 73
Wo.	15						
Mgte.	.30	.81	.32	45	15	.47	.11
Sph.	.23	.97	20	.45	14	.44	08
Apte	.02	.21	.00	.04	.06	.19	.06
Femic	4.54	7.53	3.50	4.35	2.49	5.88	1.99
Mg/Fe	60/40	24/76	45/55	32/68	60/40	48/52	66/34
Plag.	Ab_{96}	Ab_{87}	Ab_{95}	Ab_{92}	Ab_{89}	Ab_{85}	Ab_{92}

* Iron calculated as in Table 1

7587: porphyritic grey rhyodacitic sill, composed of phenocrysts of quartz, orthoclase, oligoclase, and pseudomorphs of chlorite after biotite in a completely spherulitic matrix of intergrowths of feldspar and quartz and some secondary calcite, recrystallized from a glassy matrix. 7647: weakly porphyritic quartz monzonite of the Idaho Batholith. Larger crystals of orthoclase perthite and zoned oligoclase with finer grained biotite, euhedral hornblende and quartz. Texture is hypersolvus with resolved plagioclase. 7652: porphyritic rhyodacite of the Idaho Batholith. Phenocrysts of quartz, orthoclase, oligoclase and biotite in a finer grained matrix of similar composition. 7655: coarse grained quartz monzonite of the Idaho Batholith, containing orthoclase perthite, quartz, oligoclase, biotite and hornblende. 7700: Trondhjemitic gneiss within the Wallace Formation, containing quartz, oligoclase, untwinned alkali feldspar, and scarce biotite. 7768: porphyritic dacite sill, containing phenocrysts of orthoclase, oligoclase and biotite in a matrix of quartz, sericite, feldspar and epidote. 7785: quartz monzonite orthogneiss in the Wallace Formation.

The pegmatites, granitoids, diabase sills, and amphibolites are distinct chemically when plotted on variation diagrams. A comparison of the AFM and the calcium-potassium-sodium diagram of Figure 10 shows the highly differentiated nature of the granitoids and pegmatites. The pegmatites are distinctly richer in potassium than the sodium-rich granitoids. The amphibolites have Thornton and Tuttle (1960) differentiation indices in the range 20 to 24, the diabases 26 to 60, the granitoids 85 to 95, and the pegmatites 97 to 100, in order of increasing differentiation. Only the diabases show a significant range.

SUMMARY OF THE GEOCHRONOLOGY

BELT SEDIMENTATION

Beltian sedimentation must be younger than 1,650 m.y., an age obtained for the pre-Beltian basement in Montana (Giletti, 1971). Pre-Beltian granitic and gneissic rocks in central Idaho have yielded rubidium-strontium dates of 1,500 m.y. (Armstrong, 1975). The age of the lower Beltian is at least 1,325 m.y., based on a rubidium-strontium whole rock sediment isochron (Obradovich and Peterman, 1968), or at least 1,400 m.y. for a lead age obtained for galena in the Coeur d'Alene Beltian rocks (Zartman and Stacey, 1971). The lower Belt sedimentation must predate the potassium-argon and rubidium-strontium dates of approximately 1,200 m.y. for the cross-cutting diorite-gabbro Purcell Sills (Bishop, 1973), and 1,200 to 1,250 m.y. for uranium veins from the Coeur d'Alene Belt (Eckelmann and Kulp, 1957).

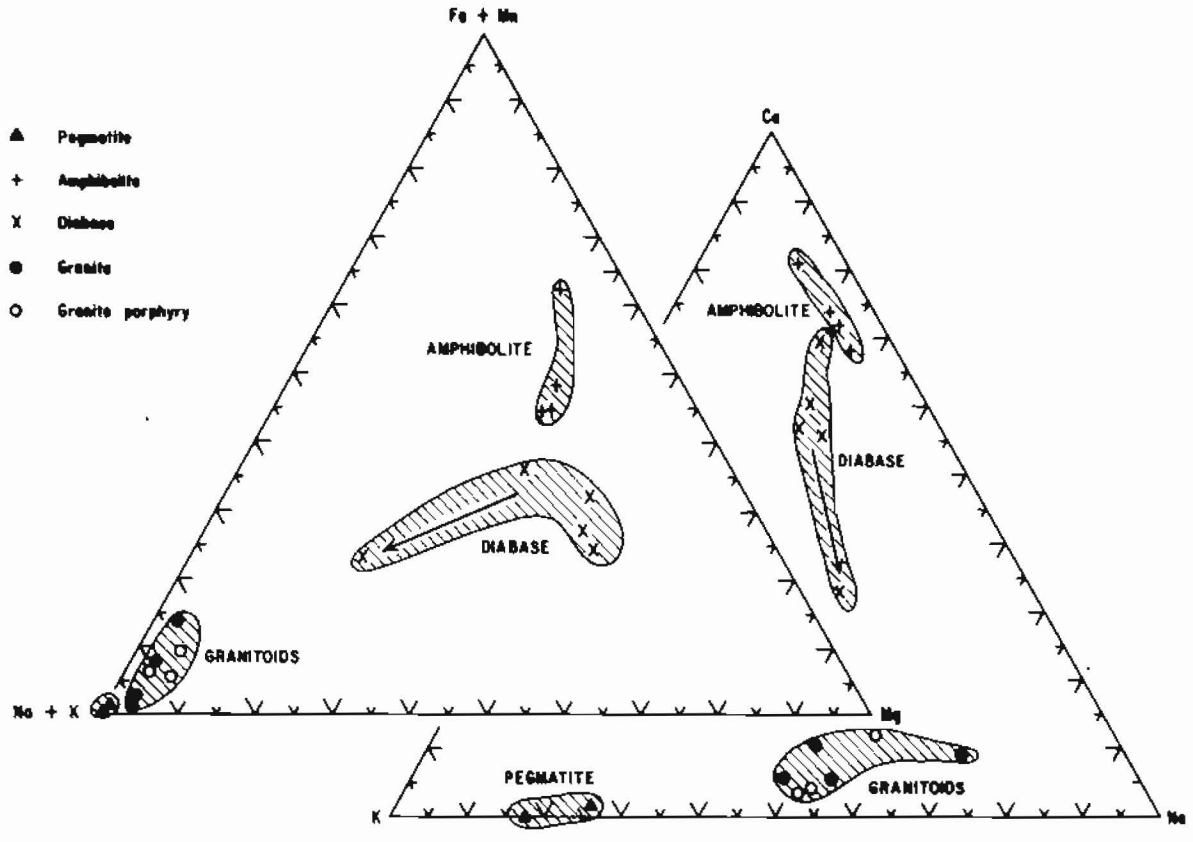

Figure 10. Plots of the igneous and meta-igneous rocks on two diagrams, showing relative cationic proportions of (Fe + Mn) vs. (Na + K) vs. (Mg) and Ca vs. K vs. Na. The arrow in the diabase field shows differentiation in a thick sill.

Rubidium-strontium dates of 1,100 and 930 m.y. for upper Belt sediments and glauconite (Obradovich and Peterman, 1968) must be taken skeptically, because of the uncertainties in sediment dating.

BELT METAMORPHISM

The metamorphic grade of the Beltian formations increases downward stratigraphically (Maxwell and Hower, 1967) and toward the Idaho batholith (Hietanen, 1963, 1967). At least part of the metamorphism occurred in the Precambrian (Eckelmann and Kulp, 1957; Bishop, 1973), and greenschist facies metamorphism prevailed in the lower Belt formations before 1,200 m.y. (Bishop, 1973). A single concordant zircon date of 950 m.y. in northern Idaho suggested to Reid and others (1973) that the East Kootenai orogeny affected northern Idaho later than 1,200 m.y. This orogeny may have extended from 1,350 to 800 m.y., but the timing is confused.

The possibility of two separate Precambrian metamorphic events affecting the Belt-Purcell rocks seems more likely. An earlier deformation, accompanied by high pressure (kyanite and sillimanite) metamorphism, was overprinted by a later, low pressure (cordierite and andalusite) metamorphism (Cheney, 1975; Reid and Greenwood, 1968). The dating of these events is strongly in doubt because of the very complex isotope data. These difficulties have been emphasized by Hofmann (1971, 1972). A severe scatter of the Sr^{87}/Sr^{86} versus the Rb^{87}/Sr^{86} whole rock data shows that most or all of the metamorphic samples were open systems after a sufficiently long time had passed to build up the observed different Sr^{87}/Sr^{86} ratios (Hofmann, 1972). The redistribution was not intense enough to homogenize the rocks isotopically on a regional scale. A sample from the sillimanite-muscovite zone gave an individual mineral isochron, showing that metamorphic

crystallization occurred at 64 m.y. A younger biotite age of 54 m.y. was caused by either slow cooling or reheating of the terrane. A specimen of garnet-bearing micaceous metaquartzite gave a mineral isochron of 340 m.y. and a biotite age of 183 m.y. The meaning of these mineral separate isochrons is uncertain.

The rubidium-strontium ages of separated biotites, ranging from 40 to 60 m.y. in the sillimanite, kyanite, and staurolite zones, increases sharply to about 200 m.y. in the garnet zone and reaches 430 m.y. in the biotite zone. A possible interpretation is that the low-grade metamorphic zones were not recrystallized in the Mesozoic-Tertiary event and that biotite crystallized during the earlier Precambrian metamorphism and then suffered partial loss of radiogenic strontium (Hofmann, 1972). The last pulse of metamorphic heating probably occurred about 45 m.y., and the data are consistent with, but do not prove, the interpretation that this event established the dominant metamorphic mineral assemblages (Hofmann, 1971).

IDAHO BATHOLITH AND RELATED ROCKS

The bulk of the Idaho batholith was emplaced during a Cretaceous culmination in igneous activity. The southern (Atlanta) lobe was emplaced about 75 to 100 m.y. and the northern (Bitterroot) lobe about 70 to 80 m.y. Much of the batholith was affected by Eocene magmatism that reset the isotopic dates to 50 m.y. or less (Armstrong and others, 1977). Initial strontium isotope ratios change abruptly from $\sim$0.7040 or less to $\sim$0.7060 or more in the east, across a boundary in western Idaho. The higher ratios imply an underlying continental crustal basement. Along the northeastern border zone of the Idaho batholith, important thermal

events have been dated: 85 ± 35 m.y. for a metamorphic event that affected quartzo-feldspathic gneiss; 82 ± 10 m.y. for the emplacement of a quartz diorite orthogneiss; 66 ± 10 m.y. for the main Idaho batholith emplacement; 46 ± 5 m.y., 42 ± 8 m.y., and 39 ± 2 m.y. for late thermal evolution of the plutons (Chase and others, 1978).

STRUCTURE

The structure of the region that controls the outcrop pattern (Figure 3; Figure 11) has resulted from two major deformations. The earliest recognizable structures are tight isoclinal F_1 folds with knife sharp crests and a well-developed axial plane schistosity which passes through the fold crests (Figure 6). The isoclinal folding is well-developed in the Burke, Revett, and St. Regis Formations. The youngest Wallace Formation was folded in the same pattern, but with less steeply dipping fold limbs and less well-developed axial plane schistosity. The intensity of compression can therefore be assumed to have increased with depth. Since the foliation is defined by biotite and muscovite, these minerals must have crystallized during the F_1 event. However, the radiometric evidence summarized above does not unambiguously define when this took place.

The structural analysis of the area is based on 940 foliation readings predominantly of the F_1 schistosity (Figure 11). The area was divided into fourteen structural domains on a trial-and-error basis (Figure 11). Most of the domains show a simple girdle on the stereogram (lower hemisphere, equal area). However, the plots of the minor fold

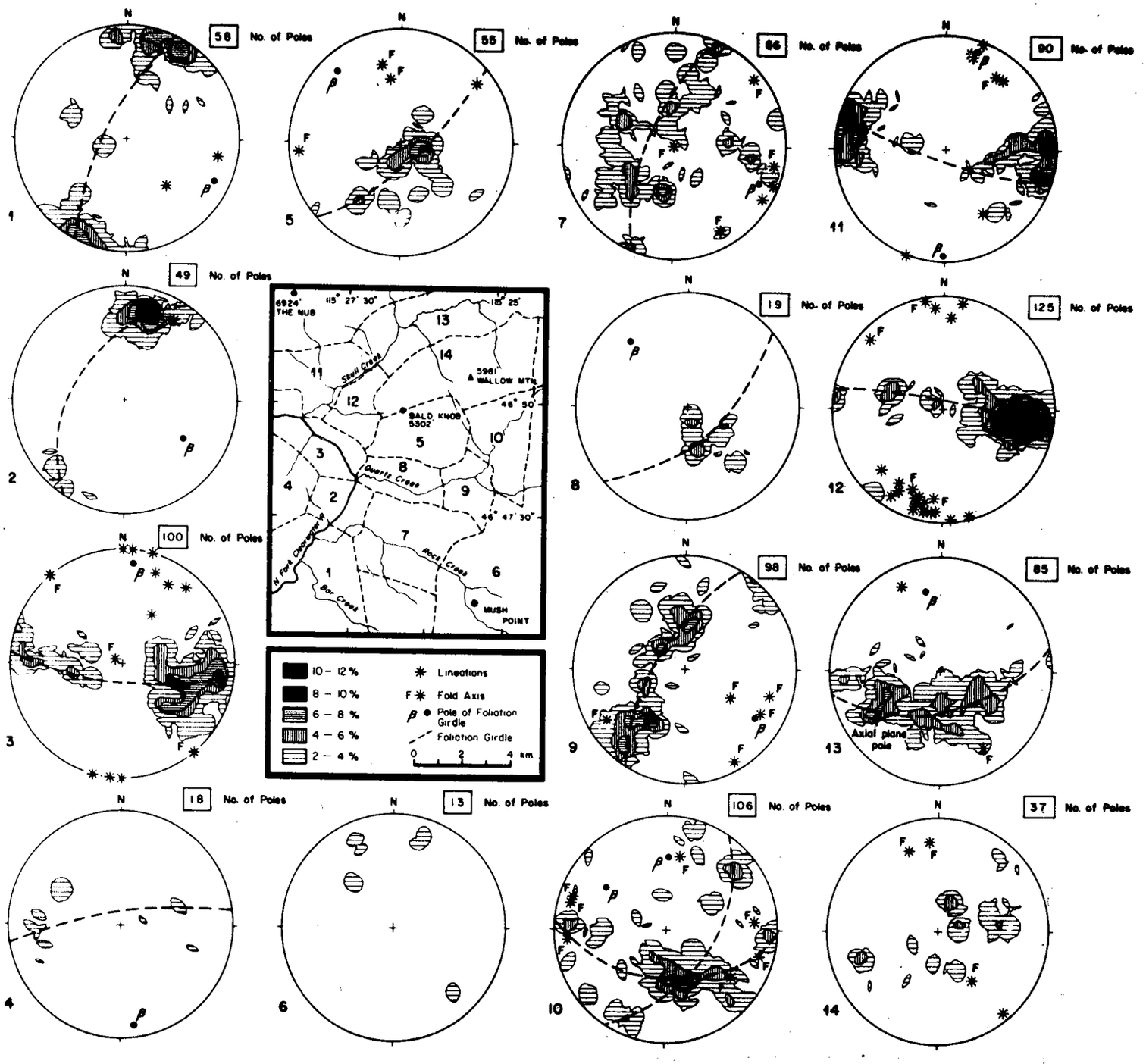

Figure 11. Structural analysis of the area, divided into fourteen domains. The stereograms are equal area, lower hemisphere projections. The locality map refers to Figure 3.

axes (F_1 and F_2) do not coincide with the pole to the F_1 girdle, as for example in domains 3, 5, 7, 9, 10, and 12. The spread of poles from a sharp girdle may be ascribed largely to the effect of refolding of the schistosity around the F_3 axis. It can be seen that even if an F_2 deformation could be proven for the area, it was indeed of minor importance in comparison with the F_1. As has been shown by outcrop study, the F_1 deformation led to a strong development of axial plane schistosity. The poles to the foliation plane girdles can therefore be taken to represent the F_1 fold axes to the nearest approximation.

The F_1 fold axes change direction and swing from a northwesterly trend to a northerly trend (Figure 11). When these trends are transferred to the geologic map (Figure 3), they clearly show that the F_1 foliation has been folded into a major late-stage open fold whose axis plunges to the northeast. The western limb of this syncline is overturned: the junction between the younger Wallace Formation and the St. Regis Formation, along Skull Creek and Pear Creek, dips to the west at about 60 degrees. The southern limb appears to have a normal stratigraphic dip (Figure 3).

The spread of fold axes requires at least three periods of noncollinear deformation. The axes are symmetrically disposed about the large late-stage synclinal F_3 axis (Figure 12). Unfolding the F_3 would move all the earlier fold axes along appropriate small circles and could be used to eliminate all the fold axes in the southeast quadrant and concentrate them predominantly in the northwest quadrant (Figure 12). The resulting dispersal of the original fold axes could then be explained by an F_2 folding phase whose axial trend lay somewhere between north to N. 50° W. But there is no unique solution for such an analysis. The data simply illustrate the need for an F_2 deformation to disperse the original F_1 fold axes.

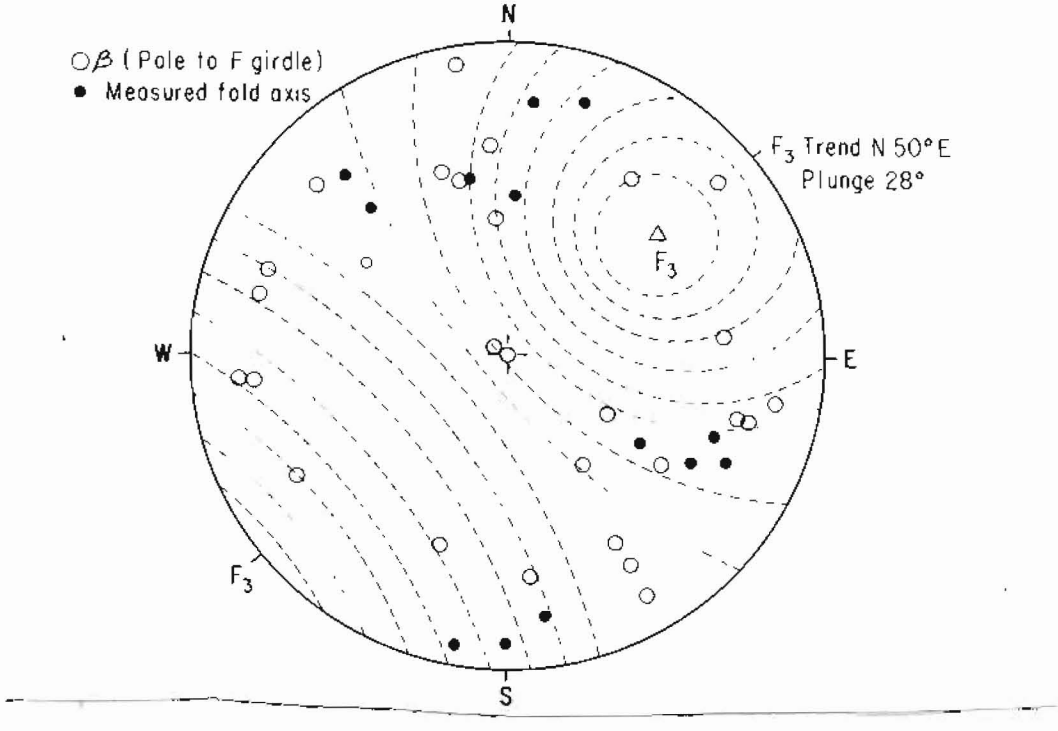

Figure 12. All the measured fold axes and poles to the foliation girdles, as deduced from Figure 11, plotted on the stereogram (lower hemisphere, equal area). The pattern of small circles is centered around the late-stage F_3 plunging fold axis.

The study of air photographs was of little help in the structural analysis, because the rocks of this region weather rapidly on exposure and the steep slopes are covered with mica-rich scree. There is hardly any resistant rock to form ridges. However, the northerly trend of the western limb of the F_3 fold can be determined from air photographs. Farther north along upper Collins Creek, a strong north-south lineament can be seen on the photographs.

Reid and Greenwood (1968) and Reid and others (1973) discerned a second generation of F_2 folds of general northwesterly trend in the St. Joe area, swinging north-south towards the east. These folds deform the F_1 schistosity. The F_2 crests are rounded and axial plane schistosity is absent or only weakly developed.

The author was unable to distinguish the F_2 folds deforming the F_1 foliation. However, the description for the F_2 folds of the St. Joe area would fit the F_1 fold style found in the Wallace Formation of the study area. The folds have rounded crests (Figure 5), and the prominent north-south axial trend continues northward as prominent features on aerial photographs. The folds in the Wallace Formation, however, have not been found to deform any pre-existent schistosity. Hence, they are interpreted as F_1 but of varying style, appropriate with the less deeply buried Wallace Formation.

OROGENIC EVOLUTION

In the St. Joe area immediately to the north, the F_1 event was interpreted as Barrovian, characterized by synkinematic recrystallization

and recumbent isoclinal folding about N. 70° W. axes. This direction is strongly preserved in the study area east of the North Fork of the Clearwater River (Figure 3; Figure 11), especially along the Moscow Bar Ridge. Within the study area, regional metamorphism was entirely sillimanite grade, and a comparison with Hietanen (1968) shows the zones progressing in a south-southwest direction from kyanite and staurolite to kyanite to kyanite and sillimanite to sillimanite and muscovite (Figure 2). The metamorphism was under a confining pressure greater than the Al_2SiO_5 triple point (Figure 13). To the north, staurolite has already broken down with increasing temperature to give kyanite, but muscovite has not yet broken down completely, even though the content of alkali feldspar has increased. The position of the line for the breakdown of staurolite (Figure 13), after Winkler (1974), is for the iron-rich variety. A less iron-rich variety would have broken down at a lower temperature.

Although the reaction accompanying the formation of sillimanite may have been accompanied by some anatexis, most of the high-grade metamorphism was synchronous with the emplacement of the main Idaho batholith and its Mesozoic precursors. Pegmatite, quartz-feldspar veins and layers, and orthogneiss that permeate the Wallace Formation may have been formed as a precursor of the Idaho batholith (Chase and others, 1978). That the granitic activity was accompanied by folding is clear, because the pegmatite layers and veins are boudinaged and folded together with the country rocks (Figure 6). Occasionally whole areas became migmatite (Figure 7). The alkali feldspar, formed at this time, was a high triclinicity microcline, as would be formed under mesozonal conditions followed by slow cooling. Water released during most of the metamorphic reactions (Figure 13) and the deformation during crystallization would

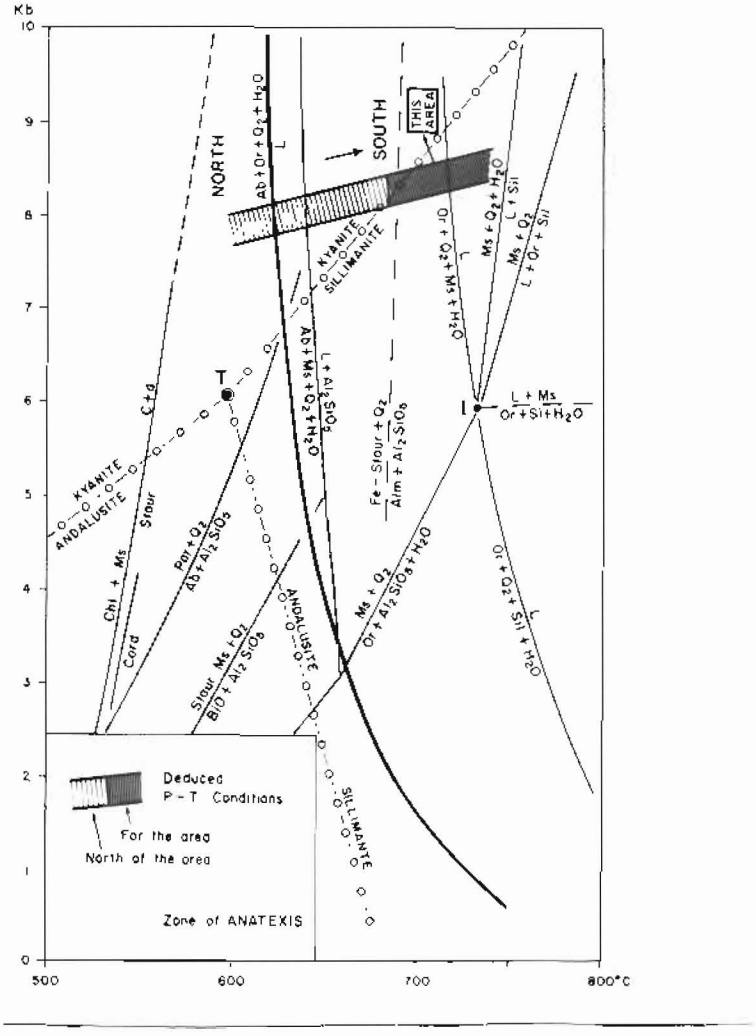

Figure 13. Pressure-temperature conditions of metamorphism of the Beltian metasedimentary formations. All stability boundaries are from Winkler (1974). The field of the study area is defined. Actual pressure depends upon the acceptance of the value for the triple point T.

have greatly facilitated attainment of the low temperature structural state by the feldspars (Yund, 1975).

Reid and Greenwood (1968) and Cheney (1975) describe the later low-pressure metamorphism that accompanied the F_2 deformation in the areas to the north. The change in geothermal gradient from the initial metamorphism is clear, because andalusite forms pseudomorphs after kyanite in the St. Joe area. The isograds of the F_2 metamorphism are not parallel to those of F_1, but both orogenies caused an increasing grade towards the south (Figure 2). By extrapolating the isograds, both orogenies would have reached sillimanite grade in the study area. Hence, it is not surprising that the two separate orogenic crystallizations could not be detected. An estimation of the time of the F_2 deformation is difficult, but the radiometric data of Hofmann (1971, 1972) strongly suggest that it was around 45 m.y. when biotite in most of the higher grade metamorphic zones recrystallized. The earlier F_1 deformation may well have been Precambrian and related to the development of the Belt-Purcell aulacogen on the North American cratonic margin, but the problem of dating the metamorphic events is not easy to resolve in view of the complicated radiometric data.

Reid and Greenwood (1968) ascribed thrust faulting and diabase sill injection to the late phases of the F_2 deformation, which they suggested was 700 m.y. However, the diabase sills of the study area are extremely young and have been neither deformed nor metamorphosed. Hence, I would ascribe an Eocene age, though no radiometric dating has been carried out.

The final late-stage F_3 deformation of a large open-fold style has deformed the F_1 isoclinal folds into a broad syncline plunging gently

toward the northeast. This folding episode is responsible for the curved outcrop pattern of the formations (Figure 3). This style of late-stage folding has not previously been described in the Clearwater National Forest. The earlier isoclinal fold axes have clearly been folded around this northeast-plunging F_3 fold axis (Figure 3; Figure 12). The conformity of the Idaho batholith with the southern limb of the F_3 fold (Figure 3) might suggest that the F_3 deformation was approximately synchronous with the batholith emplacement or with the Bungalow pluton in the Tertiary.

The Bitterroot lobe of the Idaho batholith was emplaced into the Belt terrane at about 70 to 80 m.y. It was a relatively high level pluton whose alkali feldspar is characteristically monoclinic orthoclase. No contact metamorphic effect on the Beltian rocks has been discerned, except perhaps the shimmering with sericite of the sillimanite and garnet near the batholith at Mush Point.

The rhyodacite sills, which are widely found within the marginal areas of the batholith and within the Beltian metasediments, may be considered as Eocene and as an important period of late-stage activity within the Idaho batholith that has largely reset the older radiometric dates.

The Mesozoic-Cenozoic orogenic activity is related to the convergence and subduction of the Pacific plate beneath the North American craton. The effects of this convergence have largely obliterated the Precambrian metamorphic history associated with the separation of North America from Siberia and the development of the Belt-Purcell aulacogen.

ACKNOWLEDGMENTS

I wish to thank Rolland R. Reid and the Idaho Bureau of Mines and Geology for the use of a vehicle in the summer of 1970. Thanks are due to the rangers and staff of Bungalow and Canyon ranger stations for their help, especially to Earl Reinsel. I wish to thank Charles J. Smiley for his help, and my colleague K. R. Chakraborty for many useful discussions.

REFERENCES

Armstrong, R. L., 1975, Precambrian (1,500 m.y. old) rocks of central Idaho--the Salmon River Arch and its role in Cordilleran sedimentation and tectonics: American Journal of Science, v. 275A, p. 437-467.

Armstrong, R. L., W. H. Taubeneck, and P. O. Hales, 1977, Rb-Sr and K-Ar geochronometry of Mesozoic granitic rocks and their Sr isotopic composition, Oregon, Washington, and Idaho: Geological Society of America Bulletin 88, p. 397-411.

Bishop, D. T., 1973, Petrology and geochemistry of the Purcell Sills in Boundary County, Idaho, in Belt Symposium, v. 2, Idaho Bureau of Mines and Geology Special Report 3, p. 16-66.

Chase, R. B., M. E. Bickford, and S. E. Tripp, 1978, Rb-Sr and U-Pb isotopic studies of the northeastern Idaho batholith and border zone: Geological Society of America Bulletin 89, p. 1325-1334.

Cheney, J. T., 1975, Kyanite, sillimanite, phlogopite, cordierite layers in the Bass Creek anorthosites, Bitterroot Range, western Montana: Northwestern Geology, v. 4, p. 77-82.

Eckelmann, W. R. and J. L. Kulp, 1957, Uranium-lead method of age determination, Part II, North American localities: Geological Society of America Bulletin 68, p. 117-1140.

Giletti, B. J., 1971, Discordant isotopic ages and excess argon in biotites: Earth and Planetary Science Letters, v. 10, p. 157-164.

Goldsmith, J. R. and F. Laves, 1954, The microcline-sanidine stability relations: Geochim. Cosmochim. Acta, 5, p. 1-19.

Guild, P. W., 1978, Metallogenesis in the western United States: Journal of the Geological Society of London 135, p. 355-376.

Harrison, J. E., A. B. Griggs, and J. D. Wells, 1974, Tectonic features of the Precambrian Belt basin and their influence on post-Belt structures: U. S. Geological Survey Professional Paper 866, 15 p.

Hietanen, Anna, 1963, Idaho batholith near Pierce and Bungalow, Clearwater County, Idaho: U. S. Geological Survey Professional Paper 344-D, p. D1-D42.

--------, 1967, Scapolite in the Belt Series in the St. Joe-Clearwater region, Idaho: Geological Society of America Special Paper 86, 56 p.

--------, 1968, Belt Series in the region around Snow Peak and Mallard Peak, Idaho: metamorphic and igneous rocks along the northwest border zone of the Idaho batholith: U. S. Geological Survey Professional Paper 344-E, p. E1-E34.

--------, 1969, Distribution of Fe and Mg between garnet staurolite and biotite in aluminum rich schist in various metamorphic zones north of the Idaho batholith: American Journal of Science, v. 267, p. 422-456.

Hobbs, S. W. and V. C. Fryklund, Jr., 1968, The Coeur d'Alene district, Idaho, in J. D. Ridge, editor, Ore Deposits of the United States, 1933-1967, v. II: American Institute of Mining Metallurgical Petroleum Engineers, New York, p. 1417-1435.

Hofmann, A., 1971, Effect of regional metamorphism on radiometric ages in pelitic rocks--preliminary results: Annual Report of the Director of the Geophysical Laboratory, Carnegie Institution, 1970-1971, p. 242-245.

--------, 1972, Effect of regional metamorphism on the behaviour of Rb and Sr in micas and whole-rock systems of the Belt Series, northern Idaho: Annual Report of the Director of the Geophysical Laboratory, Carnegie Institution, 1971-1972, p. 559-563.

Hutchison, C. S., 1974, Laboratory Handbook of Petrographic Techniques: John Wiley-Interscience, New York, 527 p.

--------, 1975a, A systematic programme for the X-ray fluorescence analysis of rocks and minerals: Warta Geological Newsletter of the Geological Society of Malaysia, v. 1, p. 1-4.

--------, 1975b, The norm, its variations, their calculation and relationships: Schweiz. Mineral. Petrogr. Mitt., 55, p. 243-256.

Maxwell, D. T. and J. Hower, 1967, High-grade diagenesis and low-grade metamorphism of illite in the Precambrian Belt series: American Mineralogist, v. 52, p. 843-956.

Norrish, K. and J. T. Hutton, 1969, An accurate X-ray spectrographic method for the analysis of a wide range of geological samples: Geochim. Cosmochim. Acta, 33, p. 431-453.

Obradovich, J. D. and Z. E. Peterman, 1968, Geochronology of the Belt Series, Montana: Canadian Journal of Earth Science, v. 5, p. 737-747.

Powder Data File, 1974, Selected Powder Diffraction Data for Minerals, Data Book: Joint Committee for Powder Diffraction Standards, Pennsylvania, 833 p.

Reid, R. R. and W. R. Greenwood, 1968, Multiple deformation and associated progressive polymetamorphism in the Beltian rocks north of the Idaho batholith, Idaho, U.S.A.: 23rd International Geological Congress, v. 4, p. 75-87.

Reid, R. R., D. A. Morrison, and W. R. Greenwood, 1973, The Clearwater orogenic zone: a relict of Proterozoic orogeny in central and northern Idaho, in Belt Symposium, v. 1: Idaho Bureau of Mines and Geology Special Report 2, p. 10-56.

Ross, C. P., 1970, The Precambrian of the United States of America: Northwestern United States--the Belt Series, in K. Rankama, editor, Precambrian, v. 4, John Wiley-Interscience, New York, p. 145-251.

Sears, J. W. and R. A. Price, 1978, The Siberian connection: a case for Precambrian separation of the North America and Siberia cratons: Geology, v. 6, p. 267-270.

Stewart, D. B., 1975, Lattice parameters, composition, and Al/Si order in alkali feldspars, in P. H. Ribbe, editor, Feldspar Mineralogy, Mineralogical Society of America, Short Course Notes, v. 2, p. St-1 - St-22.

Stewart, J. H., 1976, Late Precambrian evolution of North America: plate tectonics implication: Geology, v. 4, no. 1, p. 11-15.

Streckeisen, A., 1976, To each plutonic rock its proper name: Earth Science Reviews, v. 12, p. 1-33.

Swanberg, C. A. and B. D. Blackwell, 1973, Area distribution and geophysical significance of heat generation in the Idaho batholith and adjacent intrusions in eastern Oregon and western Montana: Geological Society of America Bulletin, v. 84, p. 1261-1282.

Thornton, C. P. and O. F. Tuttle, 1960, Chemistry of igneous rocks, I differentiation index: American Journal of Science, v. 258, p. 664-684.

Tuttle, O. F. and N. L. Bowen, 1958, Origin of granite in the light of experimental studies in the system $NaAlSi_3O_8$ -$KAlSi_3O_8$ -SiO_2-H_2O: Geological Society of America Memoir 74, 153 p.

Winkler, H. G. F., 1974, Petrogenesis of Metamorphic Rocks, third edition: (Translation by E. Froese), Springer-Verlag, Berlin, 320 p.

Wright, T. L., 1968, X-ray and optical study of alkali feldspars: an X-ray method for determining the composition and structural state from measurement of 2θ values for three reflections: American Mineralogist, v. 53, p. 88-104.

Yund, R. A., 1975, Microstructure, kinetics, and mechanisms of alkali feldspar exsolution, in P. H. Ribbe, editor, Feldspar Mineralogy: Mineralogical Society of America, Short Course Notes, v. 2, p. Y29-Y57.

Zartman, R. E. and J. S. Stacey, 1971, Lead isotopes and mineralization ages in Belt Supergroup rocks, northwestern Montana and northern Idaho: Economic Geology, v. 66, p. 849-860.